

P333 TUMOR TARGETING PROPERTIES OF ^{203}Pb -DOTA-Re(Arg¹¹)CCMSH IN A B16/F1 MURINE MELANOMA-BEARING MOUSE MODEL

Y. MIAO¹, D.R. FISHER², H.A. MOORE³, R.F. TESTA³ and T.P. QUINN^{4,5}

¹College of Pharmacy, University of New Mexico, Albuquerque, NM, USA; ²Pacific Northwest National Laboratory, Richland, WA, USA; ³AlphaMed Inc., Acton, MA, USA; ⁴Departments of Biochemistry and Radiology, University of Missouri-Columbia, Columbia, MO, USA; ⁵Department of Veterans Affairs Medical Center, Columbia, MO, USA

Introduction: ^{212}Pb -DOTA-Re(Arg¹¹)CCMSH appeared to be a novel effective radiopharmaceutical for melanoma treatment. Forty-five percent of B16/F1 murine melanoma-bearing C57 mice survived an 120-day study disease free after the treatment of 200 mCi of ^{212}Pb -DOTA-Re(Arg¹¹)CCMSH. However, there is a need to develop an imaging surrogate of ^{212}Pb -DOTA-Re(Arg¹¹)CCMSH to monitor the tumor response to ^{212}Pb -DOTA-Re(Arg¹¹)CCMSH treatment since ^{212}Pb is not an ideal imaging isotope. The purpose of this study was to evaluate the biodistribution of ^{203}Pb -DOTA-Re(Arg¹¹)CCMSH as an imaging surrogate of ^{212}Pb -DOTA-Re(Arg¹¹)CCMSH.

Experimental: DOTA-Re(Arg¹¹)CCMSH was labeled with ^{203}Pb in 0.5 M NH₄OAc buffer at pH 5.4. The internalization and efflux of ^{203}Pb -DOTA-Re(Arg¹¹)CCMSH was determined in B16/F1 murine melanoma cells. The pharmacokinetics of ^{203}Pb -DOTA-Re(Arg¹¹)CCMSH was examined in B16/F1 melanoma-bearing C57 mice.

Results and Discussion: ^{203}Pb -DOTA-Re(Arg¹¹)CCMSH was easily prepared in NH₄OAc buffer and completely separated from the excess non-radiolabeled peptide by RP-HPLC. ^{203}Pb -DOTA-Re(Arg¹¹)CCMSH displayed fast internalization and long retention in B16/F1 cells. Approximately 73% of ^{203}Pb -DOTA-Re(Arg¹¹)CCMSH activity internalized after a 20-min incubation at 25°C. After incubating the cells in culture media for 20 min, 78% of internalized activity remained in the cells. ^{203}Pb -DOTA-Re(Arg¹¹)CCMSH exhibited similar biodistribution pattern with ^{212}Pb -DOTA-Re(Arg¹¹)CCMSH in B16/F1 melanoma-bearing mice. ^{203}Pb -DOTA-Re(Arg¹¹)CCMSH displayed receptor-mediated tumor uptake of $11.87 \pm 3.24\% \text{ID/g}$ at 2 h post-injection. Non-target organ uptakes were considerably low ($<1.11\% \text{ID/g}$) except for the kidneys at 2, 4 and 24 h post-injection. The renal uptake was $7.78 \pm 1.42\% \text{ID/g}$ at 2 h post-injection. The whole-body clearance of ^{203}Pb -DOTA-Re(Arg¹¹)CCMSH was fast, with approximately 89% of the activity cleared through urinary system by 2 h post-injection.

Conclusion: Favorable pharmacokinetics of ^{203}Pb -DOTA-Re(Arg¹¹)CCMSH highlighted its potential as a novel matched-pair imaging agent to monitor the tumor response to ^{212}Pb -DOTA-Re(Arg¹¹)CCMSH treatment.

Keywords: Melanoma Targeting, ^{203}Pb Labeled, Alpha-Melanocyte Stimulating Hormone Peptide

P334 EXPERIMENTAL HYPOXIA AS A POTENT STIMULUS FOR RADIOTRACER UPTAKE IN VITRO: COMPARISON OF DIFFERENT TUMOR CELLS AND PRIMARY ENDOTHELIAL CELLS**F. TREITE¹, J. OSWALD¹, C. HAASE¹, P. MAEDING², B. SCHWENZER³, R. BERGMANN¹ and J. PIETZSCH¹**

¹Radiopharmaceutical Biology, Institute of Radiopharmacy, Research Center Dresden-Rossendorf, Dresden, Germany; ²Radiopharmaceutical Chemistry, Institute of Radiopharmacy, Research Center Dresden-Rossendorf, Dresden, Germany; ³Institute of Biochemistry, Technical University Dresden, Dresden, Germany

Introduction: Hypoxia is a common feature of solid malignant tumors. The vascular endothelial growth factor (VEGF) is upregulated by hypoxia inducible factors (HIFs) as a result of central hypoxia and plays an outstanding role for the formation of new tumoral blood vessels by promoting proliferation and migration of endothelial cells. Beside [¹⁸F]fluorodeoxyglucose (18F-FDG) as standard radiotracer for tumor imaging with PET, oxygenation status in experimental and human tumors can be visualized by using [¹⁸F]fluoromisonidazole (18F-FMISO).

Experimental: The aim of our study was the evaluation of the uptake of the radiotracers 18F-FDG and 18F-FMISO under standardized hypoxic conditions in various primary endothelial cells compared with three tumor cell lines in vitro. Experimental hypoxia was characterized by measurement of expression of HIF-1 α , VEGF and various VEGF receptors by quantitative real-time PCR.

Results and Discussion: Experimental hypoxia was confirmed by significant upregulation of characteristic hypoxia-related genes like VEGF in all analyzed primary endothelial cells and the tumor cell lines. VEGF receptors 1, 2 and 3 were almost absent in tumor cells and only expressed in endothelial cells. In contrast, the VEGF co-receptor Neuropilin-1 showed an increased expression in tumor cells under experimental hypoxia. In comparison to normoxic conditions, cellular uptake of 18F-FDG was significantly increased under experimental hypoxia in both tumor and endothelial cells. Otherwise, uptake of 18F-FMISO was always higher in tumor cells than in endothelial cells under hypoxic conditions.

Conclusion: Our data showed a strong dependence of 18F-FDG uptake on the availability of oxygen in vitro. The study demonstrates relevance of endothelial cells as one important part of the tumor microenvironment under hypoxic conditions. This may have implications when performing PET studies aiming at the visualization and characterization of highly vascularized tumors, in particular, when using 18F-FDG.

Keywords: 18F-FMISO, 18F-FDG, Vascular Endothelial Growth Factor

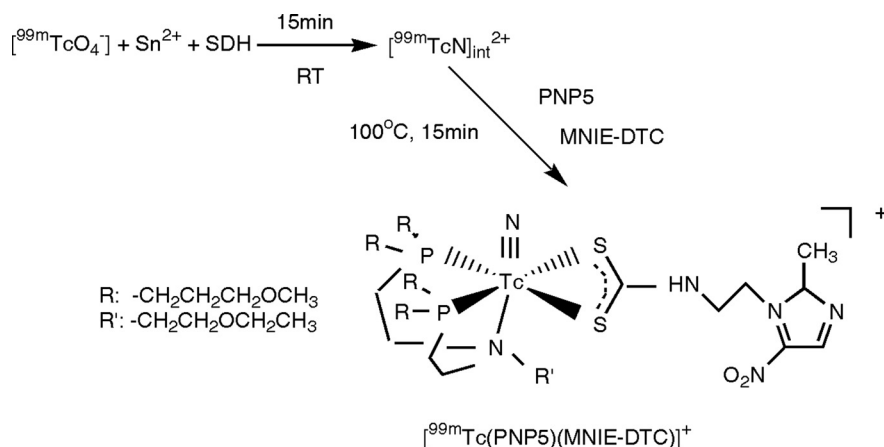
P335 SYNTHESIS AND BIOLOGICAL EVALUATION OF A NOVEL ASYMMETRICAL ^{99m}Tc -NITRIDO COMPLEX OF METRONIDAZOLE DERIVATIVE

D. KONG, J. LU, S. YE and X. WANG

Key Laboratory of Radiopharmaceuticals of Ministry of Education; College of Chemistry, Beijing Normal University, Beijing, China

Introduction: Many radiolabeled nitroimidazole-containing compounds have been developed for tumor hypoxia imaging agent. The lipophilicity of these compounds appears to play a significant role. Recently, a series of asymmetrical hetero-complexes of the type $[\text{}^{99m}\text{TcN}(\text{PNP})(\text{XY})]^{+0}$ reported by Bolzati and his coworkers have been used in the development of new radiopharmaceuticals. The ether groups of the PNP5 ligand can modify the lipophilicity of ^{99m}Tc -nitrido hetero-complexes. Hence in this study, in order to develop a new hypoxia imaging agent, a new dithiocarbamate ligand, potassium 2-(2-methyl-5-nitro-1H-imidazolyl)-ethyl-carbamate (MNIE-DTC) was designed and synthesized as the bidentate ligands to react with $[\text{}^{99m}\text{TcN}(\text{PNP5})]^{2+}$ to obtain the asymmetrical ^{99m}Tc -nitro complex.

Experimental: The corresponding ^{99m}Tc -complex had been successfully obtained by addition of N-Ethoxyethyl-N,N-bis[2-(bis(3-methoxypropyl)phosphino)ethyl]-amine (PNP5) and the dithiocarbamate ligand to the ^{99m}Tc -nitro precursor solution at 100°C for 15 min. The radiochemical purity of the product was above 95% as measured by TLC and HPLC. Biological evaluation of $[\text{}^{99m}\text{TcN}(\text{PNP})(\text{MNIE-DTC})]^+$ was performed in Kunming mice bearing H22 tumor.



Scheme 1. Synthesis of the complex $[\text{}^{99m}\text{TcN}(\text{PNP})(\text{MNIE-DTC})]^+$.

Results and Discussion: Biodistribution showed that the complex had a selective accumulation ($0.57 \pm 0.06\%$ ID/g at 1h) and good retention ($0.43 \pm 0.09\%$ ID/g at 4h) in tumor. The ratios of tumor/blood and tumor/muscle rose with time and were 2.46 and 1.31 at 1 h p.i., and reached 4.52 and 2.86 at 4 h p.i., respectively. Compared with other ^{99m}Tc -labeled nitroimidazoles, such as ^{99m}Tc -BMS181321 and ^{99m}Tc -BRU59-21, the complex showed a far lower uptake in liver and a higher tumor/blood ratio (Table 1). It was probably due to the low lipophilicity of this complex, resulting in lower liver uptake and fast plasma clearance.

Table 1. Comparison of biological characteristics of $[\text{}^{99m}\text{TcN}(\text{PNP})(\text{MNIE-DTC})]^+$ with earlier reported agents at 2h p.i. (Note: P is the partition coefficient)

Complex	$[\text{}^{99m}\text{TcN}(\text{PNP})(\text{MNIE-DTC})]^+$	^{99m}Tc -BMS181321	^{99m}Tc -BRU59-21
P	7.37	40	12
Tumor (%ID/g)	0.45 ± 0.05	0.55 ± 0.08	0.37 ± 0.14
Liver (%ID/g)	1.74 ± 0.41	8.79 ± 3.05	8.37 ± 0.87
Tumor/Muscle	2.32	2.63	3.84
Tumor/Blood	3.09	0.31	0.86
Tumor model	H22	KTH-C	KTH-C

Conclusion: The complex $[\text{}^{99m}\text{TcN}(\text{PNP5})(\text{MNIE-DTC})]^+$ is a very promising candidate for further research as a hypoxia- imaging agent.

Keywords: Hypoxia, ^{99m}Tc -Nitrido Complex, Biodistribution

P336 ENANTIOMERIC FORM OF FMISO IS NOT CRITICAL FOR HYPOXIA IMAGING

L.M. PETERSON, M. MUZI, T.C.H. ADAMSEN, J.M. LINK, J.G. RAJENDRAN, A.M. SPENCE, J. SCHARNHORST and K.A. KROHN

Molecular Imaging Center, University of Washington, Seattle, WA, USA

Introduction: [^{18}F]-fluoromisonidazole, FMISO, is useful for imaging hypoxia. Radiofluorination of 2R-(-)-glycidyl tosylate, GOTS, followed by reaction of epifluorohydrin with 2-nitroimidazole (J Nucl Med 1989;30:343) produces a single enantiomer. The simple displacement (Appl Radiat Isot 1993;44:1085) using NITTP (*1-(2'-nitro-1'-imidazolyl)-2-O-tetrahydropyranyl-3-O-toluenesulfonylpropanediol*) from ABX also gives a single enantiomer. We subsequently used a local synthesis of NITTP that was prepared in a higher yield but was a mixture of diastereomers (J Label Comp Radiopharm 2005;48:923). This precursor's purity was established by NMR, HPLC and MS and it was approved by our RDRC for pharmacokinetic studies to compare the racemic product with the single enantiomer. Since the nitro in FMISO is far from its stereocenter, the enantiomeric nature was not anticipated to affect biodistribution kinetics or electron affinity and retention in hypoxic cells but this hypothesis required testing.

Experimental: All preparations had comparable specific activity (~ 5 MBq/nmol) and the injected mass of FMISO was similar in each case. 260 MBq was injected IV and a static image was acquired for 20 min starting 2 hrs after administration of FMISO. A venous blood sample taken during the imaging procedure was used to convert image and blood values to Bq/cm³, to calculate a tissue-to-blood ratio, T/B, for each image voxel. The mean and standard deviation were calculated for %ID/g in blood and T/B for normal tissue.

Results and Discussion: Patients were divided into those who received product from the GOTS route (n=115), NITTP from ABX (69) or racemic NITTP (66). The patients were also divided into whether brain or muscle was the more abundant normal tissue. The mean age, weight, dose injected and imaging times were closely matched for the three groups. The significance of differences was evaluated by Students t-test.

Synthesis	Blood % ID/g (120m)	Muscle/Blood	Brain/Blood
2R-(-)-GOTS	0.00189 \pm 0.00057	0.898 \pm 0.180	0.918 \pm 0.169
NITTP/ABX	0.00184 \pm 0.00036	0.899 \pm 0.162	0.945 \pm 0.125
Racemic NITTP	0.00199 \pm 0.00043	0.852 \pm 0.077	0.970 \pm 0.074

Conclusion: These results failed to detect any differences in the blood clearance rates or the uptake ratios for the three products. The normal T/B values were tightly clustered just below one, as expected for a molecule with partition coefficient close to unity. We conclude that the diastereomer is an appropriate precursor for preparation of FMISO.

Acknowledgement: This research was supported by NCI P01 CA42045 and S10 RR17229. We thank John Grierson for help with radiosynthesis.

Keywords: Fluoromisonidazole, Chiral Radiopharmaceutical, Hypoxia Imaging, Pharmacokinetics

P337 SMALL ANIMAL PET IMAGING OF HYPOXIA – COMPARISON OF (¹⁸F)FAZA AND (⁶⁴Cu)ATSM IN TWO MOUSE TUMOR MODELS

G. REISCHL¹, B.J. PICHLER², M. KNEILLING³, F. MAIER², W. EHRlichMANN¹, M. ÜBELE¹, M. KUNTZSCH¹, C.D. CLAUSSEN² and H.-J. MACHULLA¹

¹Radiopharmacy, PET Center, University of Tübingen, Tübingen, Germany; ²Department of Radiology, University of Tübingen, Tübingen, Germany; ³Department of Dermatology, University of Tübingen, Tübingen, Germany

Introduction: This study was performed to compare [¹⁸F]FAZA ([¹⁸F]fluoro-azomycin-arabinoside), a very promising PET biomarker for detecting hypoxia [1,2] and [⁶⁴Cu]ATSM, a thiosemicarbazone derivative [3,4], as well under investigation for visualization of tumor hypoxia. Pharmacokinetics of both tracers were to be evaluated in two mouse tumor models using high resolution small animal PET.

Experimental: [¹⁸F]FAZA and [⁶⁴Cu]ATSM were synthesized according to [5] and [3] in specific activities of 50 GBq/μmol, resp. 5 GBq/μmol (> 10 MBq/μg). Transgenic mice (PyV-mT, breast cancer, endogenous model) or BALB/C mice (CT26, colon carcinoma, exogenous model) were injected with either [¹⁸F]FAZA or [⁶⁴Cu]ATSM via a catheter in the tail vein. The scanner was a Siemens MicroPET, Focus 120. Scans were performed dynamically from injection for one hour. Scans after 2 hours and 3 hours followed. After the PET scans animals were sacrificed, tumors dissected and analyzed by autoradiography and immunofluorescent detection of pimonidazole for ex vivo comparison.

Results and Discussion: Both tracers showed uptake in tumors. In tumors in the PyV-mT mice (n = 10) [¹⁸F]FAZA uptake reached a plateau after a few minutes up to 1 h ($1.91 \pm 0.78\%ID/cc$). After 1 h a significant wash-out was observed down to $1.22 \pm 0.62\%ID/cc$ at 3h). Tumor/muscle ratio increased up to 5.02 ± 2.27 at 3 h. [⁶⁴Cu]ATSM showed no wash-out within 3 h in the same tumor model (n = 5). Uptake was in the same range as for [¹⁸F]FAZA ($1.34 \pm 0.45\%ID/cc$ at 3 h). T/M ratio at 3 h was lower (4.09 ± 0.30) than for [¹⁸F]FAZA (5.02 ± 2.27). In CT26 mice [¹⁸F]FAZA uptake and T/M ratios were similar to the endogenous model (n = 9). [⁶⁴Cu]ATSM (n = 3) again showed no wash-out, but in this model uptake was much higher ($3.52 \pm 0.34\%ID/cc$, 3 h). T/M ratios at 3 h were comparable for both tracers ([¹⁸F]FAZA: 4.31 ± 1.27 ; [⁶⁴Cu]ATSM: 4.21 ± 0.57). Ex vivo autoradiography and immunofluorescent detection confirmed the PET results.

Conclusion: Both [¹⁸F]FAZA and [⁶⁴Cu]ATSM could detect tumor hypoxia in two different mouse models. [¹⁸F]FAZA showed a significant wash-out in contrast to [⁶⁴Cu]ATSM, but higher T/M ratios after 3 h. In case of [⁶⁴Cu]ATSM, tumor uptake was strongly dependent on tumor type.

References: [1] Kumar P et al., J. Label. Compd. Radiopharm. 1999, 42, 3-16. [2] Piert M et al., J. Nucl. Med. 2005, 46, 106-113. [3] Lewis JS et al., J. Nucl. Med. 1999, 40, 177-83. [4] Reischl G et al., Appl. Radiat. Isot. 2005, 62, 897-901.

Keywords: Hypoxia Imaging, [¹⁸F]FAZA, [⁶⁴Cu]ATSM, Small Animal PET

P338 (¹¹C)MELATONIN: POTENTIAL PET TRACER FOR IMAGING OF β-AMYLOID PLAQUES?H. AUDRAIN¹, M. SKOVGAARD JENSEN², M. WEST², M. SIMONSEN¹ and D. BENDER¹¹PET-Center, Aarhus University Hospital, Aarhus C, Denmark; ²Institute for Anatomy, Aarhus University, Aarhus C, Denmark

Introduction: The development of new radiotracers for *in vivo* imaging of β-amyloid plaques is highly needed for the detection of Alzheimer disease (AD) as early as possible and for the follow-up of AD treatments. The present study reports the use of [¹¹C]melatonin as a possible PET-tracer for the imaging of β-amyloid deposits in transgenic mice knowing that the hormone melatonin has the following properties: 1. neuroprotective activity against amyloid-β toxicity; 2. interaction with Aβ1-40 and Aβ1-42; 3. inhibition of the progressive formation of β-sheets and amyloid fibrils and 4. free radical scavenger (protective agent against amyloid-β injury to neurons).

Experimental: Anaesthetised [Presenilin-1 (PS1)/amyloid precursor protein (APP)] transgenic mice and wild type controls were PET scanned in a Concorde MicroPET R4 scanner after intravenous injection of [¹¹C]Melatonin (10 to 25 MBq). [¹¹C]Melatonin was prepared in high radiochemical yield and high radiochemical purity by methylation with [¹¹C]CH₃OTf in acetone in the presence of NaOH (Scheme 1).



Scheme 1

Results and Discussion: Micropet evaluation of the age dependent formation of amyloid deposits in transgenic mice compared to normal controls with the PET radioligand [¹¹C]melatonin is studied. Our preliminary results show an uptake of [¹¹C]melatonin in the brain of transgenic mice in area known to be rich in plaques (cerebral cortex). The comparison of the results with wild type mice are currently under investigation.

Conclusion: The feasibility of small animal PET scanning in the AD mice model is examined. Previous work in our laboratory with the known PIB ligand [1] showed no significant difference in ¹¹C-PIB retention between transgenic and wild type mice [2]. Development of new tracers for micropet imaging of AD is therefore necessary.

References: [1] W.E. Klunk et al., *Annals of Neurology*, 2004, 55, 306-319. [2] D. Bender et al., *results to be published*.

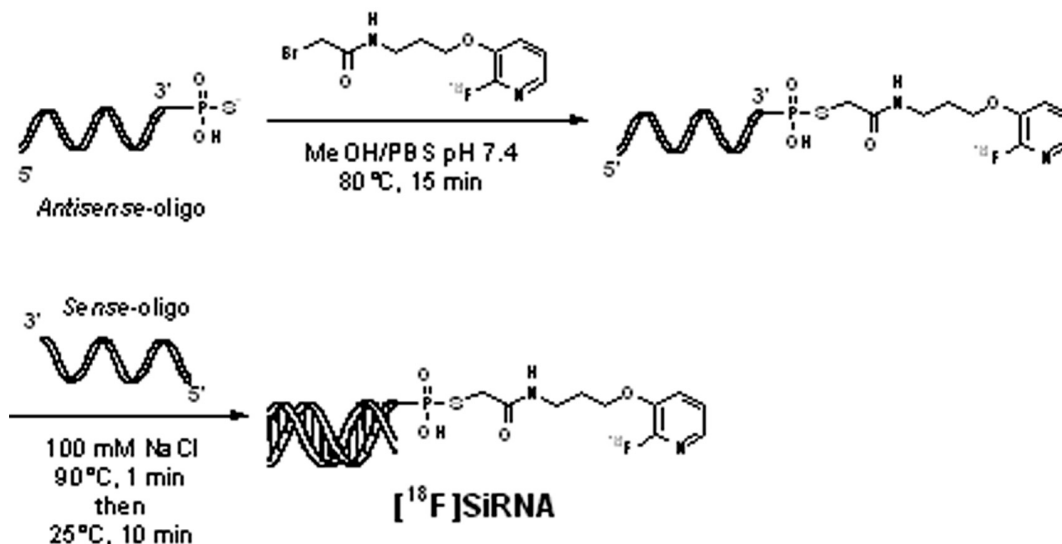
Keywords: PET, Alzheimer Disease, B-Amyloid Plaques, ¹¹C-Melatonin

P339 FLUORINE-18 LABELLING OF DOUBLE-STRANDED SMALL INTERFERING RNA

T. VIEL¹, B. KUHNAST², R. BOISGARD¹, F. HINNEN², B. TAVITIAN¹ and F. DOLLE²¹INSERM U803, CEA/DSV, Orsay, France; ²Service Hospitalier Frédéric Joliot, CEA/DSV, Orsay, France

Introduction: Small interfering RNAs (siRNA) are double-stranded oligonucleotides able to induce a specific post-transcriptional inhibition of genes. siRNA is one of the most powerful tools to achieve gene silencing in cells, but is limited *in vivo* because of the poor pharmacological properties of RNAs. In order to evaluate the *in vivo* pharmacokinetics of some selected siRNA with Positron Emission Tomography (PET), the corresponding oligonucleotide sequences have been modified in order to increase their resistance toward nucleases and then labelled with fluorine-18.

Experimental: siRNA (21 mer, non-modified or the corresponding 2'-Fluoro- and 2-OMe-modified sequences) have been labelled with fluorine using the following two-step process: (A) prosthetic conjugation of one strand with [¹⁸F]FPyBrA (Kuhnast B. et al., *Bioconj Chem*, 2004, 15 617-627), carried out in a mixture of methanol and phosphate buffer saline (pH 7.4) at 80°C for 15 min. The corresponding [¹⁸F]conjugated oligonucleotide was then HPLC-purified, desalted, and its concentration measured at 260 nm. (B) The [¹⁸F]conjugated oligonucleotide was then hybridised with its complementary strand in stoichiometric condition (in 100 mM NaCl at 90°C for 1 min and 25°C for 10 min) to give the desired [¹⁸F]conjugated siRNA. Quality controls of single- and double-stranded [¹⁸F]conjugated oligonucleotides were performed by non-denaturing polyacrylamide gel electrophoresis (PAGE) with the corresponding [¹⁹F]conjugated oligonucleotides as references, enzymatically labelled with [³²P]phosphate at their 5' end.



Results and Discussion: Typically, up to 0.55 GBq of pure [¹⁸F]conjugated siRNA can be produced in 160 min with a specific radioactivity up to 212 GBq/micromol at the end of synthesis, starting from 20.3-24.0 GBq of a [¹⁸F]fluoride batch. They were found to be at least 95% radiochemically pure. Complete hybridisation of the two strands was confirmed by non-denaturing PAGE analysis. All the [¹⁸F]conjugated siRNA have shown the same interference efficiency in cells as the non-labelled oligonucleotides.

Conclusion: The labelling procedure described above allows for the first time the study of siRNA biodistribution by PET and let to evaluate their potential of non-modified and sugar-modified siRNA.

Acknowledgement: Supported by EMIL (European Molecular Imaging Laboratories) EU contract LSH-2004-503569.

Keywords: Fluorine-18, Oligonucleotides, siRNA, Prosthetic Labelling, FPyBra

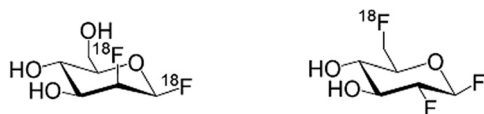
P340 FLUORINATED CARBOHYDRATES AS POTENTIAL IMAGING AGENTS FOR LYSOSOMAL STORAGE DISEASES

M.J. ADAM¹, N. LIM^{1,2}, S.G. WITHERS² and B. REMPEL²

¹PET Chemistry, TRIUMF, Vancouver, BC, Canada; ²Chemistry, University of British Columbia, Vancouver, BC, Canada

Introduction: Lysosomal storage diseases such as Tay Sachs, Gaucher and Hurler-Scheie are caused by mutations of genes encoding lysosomal hydrolases. This results in insufficient enzyme activity within the lysosome, thus an accumulation of uncleaved substrate and consequently the disease condition. The only treatment currently, enzyme replacement therapy (ERT), is extremely expensive and is only applicable to a subset of these diseases. Consequently better diagnosis and monitoring of enzyme treatments would enable more accurate dosing and allow the design of improved enzyme forms. The objective of this work was to develop PET-imaging agents to allow the quantification and localization of lysosomal enzymes in a non-invasive manner as well as to allow monitoring of enzyme replacement therapy. Reliable synthetic routes to $\{^{18}\text{F}\}2$ -fluoro-mannosyl fluoride and $\{^{18}\text{F}\}6\text{F}$ -2-fluoro-glucosyl fluoride within the short time scales imposed have been carried out.

Experimental: The 2- ^{18}F -mannosyl fluoride was synthesized in 12% radiochemical yield by the reaction of ^{18}F - F_2 with glucal in acetonitrile. Subsequent silica column chromatography was used to separate the glucose and mannose products. The 6- ^{18}F -2-fluoro-glucosyl fluoride was synthesized by the reaction of ^{18}F -fluoride with the 6-tosyl, 3,4-acetylated derivative in 85% radiochemical yield. The product was obtained after quantitative sodium methoxide deprotection. Both of these fluorinated inhibitors were allowed to incubate with Glucocerebrosidase and a model glucosidase. Binding to both of these enzymes was detected by size exclusion HPLC chromatography using a Phenomenex PolySep column.



Results and Discussion: Both F-18 labelled carbohydrate inhibitors were labeled in reasonable radiochemical yield in 1 hour after EOB. After purification both inhibitors were demonstrated to bind to either Glucocerebrosidase or a model glucosidase enzyme. Work is currently underway to optimize binding by varying the specific activity of the inhibitors and the concentration of enzyme used.

Conclusion: We have successfully labelled two glycosidase inhibitors with F-18 and demonstrated binding to two glycosidase enzymes.

Acknowledgement: We wish to thank the Natural Sciences and Engineering Research Council of Canada (NSERC) and the Canadian Institutes for Health Research (CIHR) for financial support. We also thank TRIUMF for support and the PET group personnel for assistance.

Keywords: Glycosidase, Lysosomal Storage Disease, Fluorine 18, Positron Emission Tomography, Enzyme Inhibitors

P341 SYNTHESIS AND CHARACTERIZATION OF *gem*-(¹²³I)IVACBC AS A POTENTIAL SPECT TUMOR IMAGING AGENT

W. YU, V.M. CAMP and M.M. GOODMAN

Radiology, Emory University, Atlanta, GA, USA

Introduction: 1-Amino-3-*gem*-[¹²³I]iodomethylene-cyclobutane-1-carboxylic acid (*gem*-[¹²³I]IVACBC) was synthesized and evaluated as a SPECT tumor imaging agent in 5 human cancer cell lines.

Experimental: The *gem*-IVACBC stannylated precursor was prepared in an 11 step reaction sequence from epibromohydrin. The mixture of *syn/anti*-1-[*N*-(*t*-butoxycarbonyl)amino]-3-hydroxy-cyclobutane carboxylic acid *t*-butyl esters was prepared as described earlier (McConathy *et al*, J. Appl. Rad. Isotopes, 2003, **58**, 657) with the modification of substituting *t*-butyl for methyl esters, by using Cl₃CC(=NH)*Ot*-Bu. Subsequent conversion of alcohols to the ketone by Swern oxidation followed by reaction with CHI₃/CrCl₂ followed by (Me₃Sn)₂/Pd⁰ to afford 1-[*N*-(*t*-butoxycarbonyl)amino]-3-trimethylstannylmethylene-cyclobutane carboxylic acid *t*-butyl ester as the radiolabeling precursor.

Radioiodination was carried out with no-carrier-added [¹²³I]NaI-H₂O₂/H⁺. *Gem*-[¹²³I]IVACBC was obtained by hydrolysis with TFA and chromatographic purification.

The cell assays were performed in human MDA MB468 (breast), A549 (lung), DU145 (prostate), U87 (brain) and SKOV3 (ovary) tumor cell lines in amino acid-free Dulbecco's Modified Eagle's Medium incubated for 30 minutes at 37°C, with or without inhibitors, to evaluate the compound tumor cell uptake and transport pathway. 10 mM 2-amino-bicyclo[2.2.1]-heptane-2-carboxylic acid (BCH) and 10 mM *N*-methyl- α -aminoisobutyric acid (MeAIB) were used as L- and A-type amino acid transport inhibitors, respectively.

The biodistribution study was performed in tumor-bearing SCID mice with tracer injected intravenously. The radioactivity in tumors and in normal tissues of tumor-bearing mice (n=5 each time point) was calculated at 15, 30, 60, 120 min post injection (*p.i.*) and normalized as percent injected dose per gram tissue (%ID/g).

Results and Discussion: The radiolabeling yield was 34±18% (n=7), with radiochemical purity over 99% as measured by radiometric TLC.

The cell uptake of *gem*-[¹²³I]IVACBC was measured in percent CPM per million cells relative to standard (%CPM/1×10⁶ cells), 2.1-7.2 without inhibitors. While MeAIB inhibition was not observed, significant BCH inhibition (greater than 95%) was occurred in all cases. These results suggested that *gem*-IVACBC entered tested cells primarily via L-type amino acid transport systems *in vitro*.

Gem-[¹²³I]IVACBC uptake in tumor and in muscle at 60 min *p.i.* was reported in the Table. Low uptake was found in blood, liver, bone and thyroid.

	MDA MB468	A549	DU145	U87	SKOV3
Tumor	4.3	10.4	5.4	4.1	8.0
Muscle	3.5	3.7	4.6	2.8	4.4
Tumor/Muscle	1.2	2.8	1.2	1.5	1.8

Conclusion: These findings support the candidacy of *gem*-[¹²³I]IVACBC as a SPECT tumor imaging agent.

Acknowledgement: Research sponsored by Nihon Medi-Physics. Emory University and Mark M. Goodman, PhD, are eligible for royalties from this technology.

Keywords: Amino Acids, [I-123] SPECT, Tumor Imaging

P342 COMPARATIVE IN VITRO EVALUATION OF THE HYPOXIA MARKER (^{18}F)FAZA VS. (^{18}F)FMISO

G. REISCHL, A. SABBAH and H.-J. MACHULLA

Radiopharmacy, PET Center, University of Tübingen, Tübingen, Germany

Introduction: [^{18}F]FAZA is a very promising PET biomarker for visualization of hypoxia in vivo. To date [^{18}F]FAZA has been investigated in small animal PET studies [1,2] and showed advantages over [^{18}F]FMISO, the most widely used hypoxia PET tracer. The advantages were explained by a better clearance due to higher hydrophilicity of [^{18}F]FAZA. A first in vitro study showed comparable results for both markers using rat tumor cells [3]. Here, [^{18}F]FAZA was to be further evaluated in comparison with [^{18}F]FMISO using different human tumor cell lines.

Experimental: Normal (human lung fibroblasts, CCD 32Lu (**A**)) and tumor cells (human lung carcinoma, A549 (**B**); human uterus carcinoma, SiHa (**C**)) were seeded 10^6 cells/bottle in 25 ml bottles and treated with 0.5 MBq/bottle of [^{18}F]FMISO or [^{18}F]FAZA. Cells were under an atmosphere either of room air (normoxia) or 3.5% of O_2 , 7.0% of CO_2 , 89.5% of N_2 (hypoxia) or 7.0% of CO_2 , 93% of N_2 (anoxia). After incubation at 37°C for 60, 120 and 180 min, cells were washed twice with PBS, lysed by incubation with 1 ml of trypsin in PBS for 10 min, 37°C . Intracellular activities were measured in a well-counter. Cells were tested for viability after 180 min. All experiments were $n = 3$, each value was determined 3 times.

Results and Discussion: Uptake (results calculated for 10^6 cells in %dose; mean \pm SD) was substantially higher in tumor cells than in normal cells for both tracers at 180 min under hypoxic conditions ([^{18}F]FAZA: **B**; 0.14 ± 0.02 , **A**; 0.04 ± 0.00 ; [^{18}F]FMISO: **B**; 0.12 ± 0.01 , **A**; 0.04 ± 0.01). There was little uptake under normoxic conditions (e.g. **C**, 120 min, [^{18}F]FMISO: 0.05 ± 0.01 ; [^{18}F]FAZA: 0.06 ± 0.01). Uptake was 2-3 times higher under hypoxia (**C**, 120 min, [^{18}F]FMISO: 0.10 ± 0.01 ; [^{18}F]FAZA: 0.12 ± 0.01) and under anoxia a further increase was found (**C**, 120 min, [^{18}F]FMISO: 0.16 ± 0.00 ; [^{18}F]FAZA: 0.35 ± 0.02). [^{18}F]FMISO uptake showed an increase over time (**C**; hypoxia; 60 min: 0.08 ± 0.01 ; 120 min: 0.10 ± 0.01 ; 180 min: 0.14 ± 0.00), whereas [^{18}F]FAZA uptake reached a plateau after 60 min, approximately at the level of [^{18}F]FMISO uptake at 180 min (**C**; hypoxia; 60 min: 0.12 ± 0.00 ; 120 min: 0.12 ± 0.01 ; 180 min: 0.14 ± 0.02). After 180 min under hypoxic conditions there was no difference in uptake between both tracers.

Conclusion: In this in vitro study both tracers showed hypoxia-selective uptake in the investigated human cell lines. [^{18}F]FAZA showed faster uptake, which may be an advantage compared to [^{18}F]FMISO.

Reference: [1] Piert M et al., J. Nucl. Med. 2005, 46, 106-113. [2] Solomon et al., Mol. Cancer Ther. 2005, 4, 1417-1422. [3] Sorger D et al., Nucl. Med. Biol. 2003, 30, 317-326.

Keywords: [^{18}F]FAZA, [^{18}F]FMISO, Hypoxia, In Vitro Study

P343 POLYFUNCTIONAL DENDRO-CHELATES AS NEW BRAIN SPECIFIC CONTRAST AGENTS AND RADIOTRACERS**A.V. BERTIN¹, J. STEIBEL², J.-L. GALLANI¹ and D. FELDER-FLESCHE¹**

¹Groupe des Matériaux Organiques, Institut de Physique et Chimie des Matériaux de Strasbourg, Strasbourg, France; ²Institut de Physique Biologique-Laboratoire de Neuroimagerie In Vivo, Faculté de Médecine, Strasbourg, France

Introduction: The development of the current scientific techniques in medicine such as Magnetic Resonance Imaging and Nuclear Medicine improve day by day the quality of human health and life.

Neurodegenerative diseases represent the first cause of mortality in the western countries. The diagnosis of these diseases such as Alzheimer or Parkinson requires radiopharmaceuticals which are able to reach the brain by first getting through the Blood Brain Barrier (BBB).

Thus, the goal of our research is to adopt a polyfunctional strategy for the elaboration of brain-specific radiopharmaceuticals (MRI contrast agents and radiotracers for Nuclear Medicine) by means of chemical engineering and, in particular, a 'dendrimer' approach.

Experimental: For biological applications, dendrimers and especially the DENDRON building blocks are very promising as the diversity of functionalization brought by the arborescent structure simultaneously solves the problems of biocompatibility, low toxicity, large in vivo stability and specificity. Moreover, in addition to the multifunctionalization of a low molecular weight molecule, the DENDRON building blocks allow a versatility of size (according to the generation) and of physicochemical properties (hydrophilic, lipophilic). The resulting effects on stability (dendrimer effect), contrast qualities, pharmacokinetics and biodistribution of the contrast agents and radiotracers will clearly be identified.

Results and Discussion: In the field of tree-like molecules, our work is focused on the development of a new dendro-chelate based on a synthetical water soluble siderophore (a tripodal derivative bearing one bidentate ligand on each arm) able to complex ions such as Gadolinium (III) (MRI), Manganese (II) (MEMRI), and ^{99m}Tc (III) (SPEC). The arborescent PEGylated structure grafted at the focal point of the siderophore is polyfunctional as the groups grafted at its periphery are either body (brain)-specific, or receptor (dopaminergic)-specific, or allow the product to get through the BBB.

Conclusion: Our presentation will describe the synthesis of the ligands and the MEMRI and Nuclear Medicine studies carried out on the corresponding Mn (II) and ^{99m}Tc (III) complexes respectively. We will also correlate their physicochemical properties such as their solution thermodynamics to biological activity followed by NMR and Nuclear Medicine.

Acknowledgement: We would like to acknowledge Dr. J.-L. Pierre, Dr. S. Torelli, LEDSS II, Grenoble and Dr. D. Brasse, IPHC, Strasbourg for fruitful discussions and collaborations.

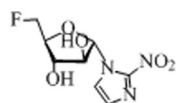
Keywords: Dendrimer, Magnetic Resonance Imaging, Nuclear Medicine, Brain Specific

P344 SYNTHESIS, TRANSPORTABILITY AND HYPOXIA SELECTIVE BINDING OF 1- β -D-(5-DEOXY-5-FLUORORIBOFURANOSYL)-2-NITROIMIDAZOLE (β -5-FAZR), A CONFIGURATIONAL ISOMER OF THE CLINICAL HYPOXIA MARKER, FAZA

P. KUMAR^{2,4}, S. EMAMI¹, J. YANG², Z. KRESOLIK², R. PAPROSKI^{3,4}, C. CASS^{3,4}, A.J.B. MCEWAN^{2,4} and L.I. WIEBE^{1,2,3}

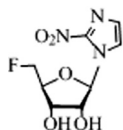
¹Faculty of Pharmacy & Pharmaceutical Sciences, University of Alberta, Edmonton; ²Oncologic Imaging; ³Department of Experimental Oncology; ⁴Oncology, Cross Cancer Institute, Edmonton, AB, Canada

Introduction: Cellular uptake of azomycin based radiosensitizers depends on perfusion and diffusion, rather than on active transport into the hypoxic cell. Image contrast with radiolabeled azomycins depends on their diffusion from normoxic tissues and renal clearance from the central compartment. [¹⁸F]FAZA, an azomycin α -nucleoside hypoxia PET marker, is under clinical evaluation world-wide and provides superior image contrast due to its faster clearance from blood than [¹⁸F]FMISO. *In vivo* PET imaging with [¹⁸F]FAZA showed that treatment response to gefitinib in A431 xenografts depends on the level of hypoxia, demonstrating its utility in assessing hypoxia as part of a therapy protocol.



FAZA

Experimental: β -5-FAZR (44%), a β -ribose analog of FAZA, is developed to exploit its transportation across cell membranes to improve uptake and contrast in hypoxic regions.



β -5-FAZR

Results and Discussion: *In vitro* radiosensitization study of β -5-FAZR in hypoxic and normoxic cells showed moderate radiosensitization of HCT116/100 colorectal carcinoma (OER 1.8). A comparison of β -AZR, β -5-FAZR and thymidine binding to cloned human equilibrative (hENT1 & 2) and concentrative (hCNT 1,2 & 3) nucleoside transporters, by determining their IC₅₀ values for inhibition of [³H]uridine transport into yeast expressing the respective recombinant hNTs, indicated that interaction of these transporters, except hCNT2, was 2-4 fold more sensitive to inhibition by thymidine than by AZR. Reduced interaction of β -5-FAZR for all five hNTs suggests its poor transportability into human cells in relation to 1- β -D-(ribofuranosyl)-2-nitroimidazole (β -AZR).

Conclusion: β -5-FAZR shows moderate radiosensitization potential and reduced interaction for human transporters (hENTs and hCNTs) in comparison to β -AZR.

Acknowledgement: ACB, NCI (CEC), CIHR (LIW), Min. of Health & Med. Education Iran (SE), Oncology Recruitment Award and Studentship from the AHFMR (RP).

Keywords: β -5-FAZR, FAZA, Hypoxia, Radiosensitization, Transportability

P345 CLICK-BASED RADIOTRACERS FOR THE SYNTHESIS OF ^{18}F -LABELLED OLIGONUCLEOTIDES

J.A.H. INKSTER, M.J. ADAM and T.J. RUTH

PET Group, TRIUMF, Vancouver, BC, Canada

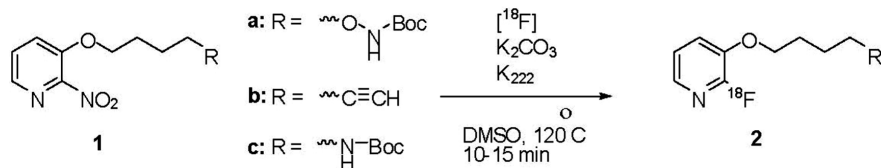
Introduction: The efficient fluorination of 2-substituted pyridinyl systems is an innovation that will likely have a major impact in the development of future prosthetic group-type ^{18}F radiotracers. 2-Bromo-N-[3-(2- ^{18}F)fluoropyridin-3-yloxy]propyl]acetamide (^{18}F -FpyBrA) couples to phosphorothioate oligonucleotides (ODNs) via 2-bromoacetamide alkylation[1]. However, in our lab and others lacking robot assistance, the long protocol reported for ^{18}F -FpyBrA (four overall steps, two HPLC purifications) remains an obstacle to routine preparations.

'Click' reactions are gaining increasing prevalence as energetically favourable linking reactions for the preparation of bioconjugates[2]. Recently, these traditionally cold labelling techniques have been used in the preparation of peptide ^{18}F -radiotracers. We seek to exploit chemoselective click reactions in the development of antisense imaging agents.

Experimental: We prepared bifunctional precursors **1a** and **1b** (analogues of ^{18}F -FpyBrA precursor **1c**) by way of Mitsunobu coupling of 2-nitro-3-hydroxypyridine with 4-[(4-boc)aminoxy]butanol and 5-hexyn-1-ol respectively.

We synthesized oxyamine-bearing **2a** and alkyne-bearing **2b** under standard $\text{K}_2\text{CO}_3/\text{K}_{222}$ conditions. Radiochemical yields were 72% and 70% respectively, as determined by radio-TLC.

We prepared a 20-mer 3'-aldehyde antisense sequence of interest via NaIO_4 oxidation of the corresponding commercial 3'-diol. We also coupled 3'-aminoethyl ODN to synthesized succinimidyl 5-azidovalerate, yielding 3'-azide material, used previously in the preparation of fluorescent DNA[3].



Results and Discussion: Compound **2a** is designed to couple with aldehyde-modified ODNs via a carbonyl addition-elimination reaction (oxime formation). Tracer **2b** (prepared in one step) is designed to couple with azide-modified ODN via a 1,3- dipolar cycloaddition reaction (1,2,3-triazole formation).

Conclusion: Two compounds bearing 2- ^{18}F fluoropyridinyl moieties tethered to 'click' functional groups were synthesized in good yield for the purposes of labeling ODNs. Corresponding modified antisense DNA was also prepared. Further experiments aimed at optimizing radiochemical yields of the bioconjugates are currently underway.

References: [1] Kuhnast, B. et al. Bioconjugate Chem. 2004, 15, 617-627. [2] Kolb, H.C.; Sharpless, K.B. Drug Discovery Today 2003, 8, 1128-1137. [3] Seo, T.S. et al. J. Org. Chem. 2003, 68, 609-612.

Acknowledgement: We thank the Canadian Institute for Health Research for their financial support.

Keywords: Antisense Imaging, Fluorine-18, Click Chemistry, Heteroaromatic Nucleophilic Substitution, Oligonucleotide Bioconjugates

P346 A POTENTIAL STEM CELL TRAFFICKING AGENT LABELED WITH ¹³¹I**D.N. PANDYA¹, H.Y. LEE¹, W. KWAK¹, J.C. PARK¹, S.-W. LEE², B.C. AHN², J. LEE² and J. YOO^{1,2}**

¹Department of Molecular Medicine, Kyungpook National University School of Medicine, Daegu, Korea; ²Department of Nuclear Medicine, Kyungpook National University School of Medicine, Daegu, Korea

Introduction: The facile and non-invasive method for stem cell trafficking is of particular interest. Recently, Kilbourn reported very simple but very effective stem cell labeling method with F-18 [Kilbourn et al., Nucl Med Biol, 2005]. Hexadecyl-4-[¹⁸F]fluorobenzoate was prepared in good yields and high purity, and was used to radiolabel mesenchymal stem cells in a yield of 25%. However, due to relatively short half-life of F-18 ($t_{1/2} = 110$ min), late microPET imaging after administration of labeled stem cell could not be obtained. Herein we report iodine analogue, hexadecyl-4-[¹³¹I]-iodobenzoate ([¹³¹I]HIB), which could be used as another good cell labeling tracer with much longer half-life ($t_{1/2} = 8$ d).

Experimental: Non-radioactive HIB was prepared by reaction of 1-hexadecanol and 4-iodobenzoylchloride in the presence of triethylamine. Then, hexabutyliditin and the catalytic amount of tetrakis(triphenylphosphine)palladium were added to a stirred solution of hexadecyl-4-iodobenzoate to give crude precursor, hexadecyl-4-(tributylstannyl)benzoate, which was further purified by column chromatography on alumina with hexane/ethyl acetate (10/1). To a mixture of precursor (100 μ g) in 100 μ L of ethyl acetate and 100 μ L of 30% H₂O₂/acetic acid (1/3 v/v) was added I-131 solution. The mixture was reacted for 10min at room temperature and then the reaction was ended by addition of 100 μ L of 0.1N HCl. The radioactive [¹³¹I]HIB was purified by HPLC with Luna C8 column (0.1% TFA/water:0.1% TFA/MeCN = 10:90).

Results and Discussion: The standard compound, HIB was prepared as a white solid in a yield of 68% and the precursor tributyltin compound was obtained as a clear colorless oil in 50% yield. Both compounds were fully characterized by ¹H and ¹³C-NMR and mass spectroscopy. The optimized labeling yield of precursor with I-131 was over 15%. The radiochemical yield of [¹³¹I]HIB after HPLC separation was determined by TLC to be 93%.

Conclusion: In conclusion, the precursor was prepared without difficulties in two step synthesis and was successfully radioiodinated with I-131 to give [¹³¹I]HIB, which is expected to be efficiently absorbed into stem cell membrane. Ongoing cell labeling study with [¹³¹I]HIB and imaging studies will be presented.

Acknowledgement: This work was supported by the Brain Korea 21 Project in 2007u.

Keywords: Stem Cell Trafficking Agent, Radioiodination, Cell Labeling, I-131

P347 SYNTHESIS AND EVALUATION OF A ^{11}C -LABELLED BETA-GALACTOSYL ESTER AS POTENTIAL PROBE FOR *IN VIVO* VISUALIZATION OF LACZ GENE EXPRESSION WITH PET

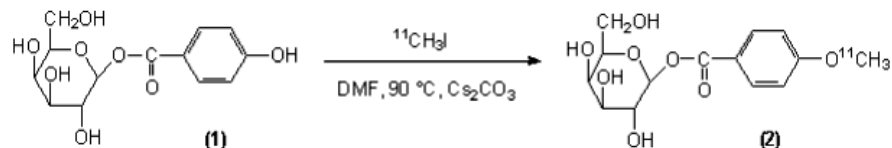
S. CELEN, T. DE GROOT, A. VERBRUGGEN and G. BORMANS

Laboratory for Radiopharmacy, K.U. Leuven, Leuven, Belgium

Introduction: Gene therapy holds great promise for the treatment of various diseases, including cancer, cystic fibrosis and immunodeficiency. A prerequisite for widespread implementation is the reliable monitoring of the transfection in a spatial and temporal way. Many promising methods are being developed to image gene expression by including a reporter gene in tandem with the therapeutic gene. One of the most widely used reporter genes is the *LacZ* gene, which encodes the bacterial beta-galactosidase enzyme. For its *in vitro* detection, several substrates are available. *In vivo* imaging of beta-gal expression would further extend the use of this reporter system.

The purpose of this study was to develop and evaluate a ^{11}C -labelled beta-gal substrate for *in vivo* visualization of *LacZ* gene expression with PET.

Experimental: Precursor (**1**) was synthesized according to a method of Schmidt and Reuss [1], who reported the synthesis of the glucosyl ester. Labelling with ^{11}C was done by alkylation of (**1**) with [^{11}C]methyl iodide in DMF at 90°C in the presence of Cs_2CO_3 . Preparative RP-HPLC purification yielded 1-[p- ^{11}C]methoxybenzoyl]-beta-galactose (**2**). Log P, *in vitro* affinity for beta-gal and biodistribution of (**2**) in mice were studied.



Results and Discussion: (**1**) was efficiently labelled with [^{11}C]methyl iodide, yielding 70% of the desired radiolabelled compound (**2**). The identity of (**2**) was confirmed by HPLC by co-elution with the authentic cold ligand. (**2**) has a log P value of -0.39. HPLC analysis after *in vitro* incubation of (**2**) for 20 min with beta-gal showed the formation of 70% of p- ^{11}C methoxybenzoic acid. Biodistribution studies in normal mice revealed negligible brain uptake at 2 min and 60 min p.i. Clearance from blood was 9.94 and occurred through the renal pathway with 76% of injected dose in the urinary bladder at 60 min p.i.

Conclusion: A beta-galactosyl ester of p-hydroxybenzoic acid (**1**) was synthesized, labelled with [^{11}C]methyl iodide and evaluated as potential probe for *in vivo* visualization of *LacZ* gene expression with PET. In an *in vitro* test, (**2**) was found to be a good substrate of beta-gal. After IV injection in mice, (**2**) showed low brain uptake and efficient excretion via the kidneys. Work is in progress to evaluate the *in vivo* stability and the *in vitro* uptake in *LacZ* expressing cells.

[1] Schmidt O.T. und Reuss H. *Liebigs Ann. Chem.* (1961)

Acknowledgement: This study was funded in part by the EC - FP6-project DiMI, LSHB-CT-2005-512146.

Keywords: PET, Carbon-11, LacZ, Beta-Gal

P348 COMPARISON OF Tc-UBI 19-41, F-UBI 19-41 AND F-UBI 18-41 IN PERIPHERAL ABSCESES USING DUAL-TRACER AUTORADIOGRAPHY IN RATS

D. SALBER¹, J. GUNAWAN³, K.J. LANGEN², W. BURCHERT³ and S. ZIJLSTRA³

¹C. & O. Vogt Institute of Brain Research, Düsseldorf University Hospital, Düsseldorf, Germany; ²Institute of Neurosciences and Biophysics-Medicine, Forschungszentrum Jülich, GmbH, Jülich, Germany; ³Institute of Molecular Biophysics, Radiopharmacy and Nuclear Medicine, Heart and Diabetes Center North Rhine-Westphalia, Bad Oeynhausen, Germany

Introduction: ^{99m}Tc-labeled peptide ubiquicidine (Tc-UBI 19-41) is under clinical evaluation for the discrimination of bacterial infection and unpecific inflammation. In this experimental study we analysed the uptake of Tc-UBI 19-41 and two ¹⁸F-labeled UBI derivatives in muscle abscesses of rats in comparison with [³H]-deoxyglucose (H-DG) using dual-tracer-autoradiography.

Experimental: Muscle abscesses were induced in 15 CDF-Fischer rats after inoculation of a suspension of staphylococcus aureus into the musculus tibialis anterior. One to six days later either Tc-UBI 19-41 and H-DG (n=4), F-UBI 19-41 and H-DG (n=5) or F-UBI 18-41 and H-DG (n=6) were injected simultaneously. One hour after tracer injection the rats were sacrificed, the abscess-bearing muscles removed and frozen at -50°C in isopentane. 20 µm thick cryosections were prepared and exposed first to ³H-insensitive photoimager plates to measure the distribution of Tc-UBI 19-41, F-UBI 19-41 and F-UBI 18-41 respectively. After decay of ^{99m}Tc or ¹⁸F the distribution of H-DG was determined. The autoradiograms were evaluated by regions of interest (ROIs) placed on areas with maximal tracer uptake in the abscess and in normal appearing muscle tissue. Lesion to muscle ratios (L/B) were calculated by dividing the maximal uptake in the lesion and by the mean uptake in the muscle tissue. For histological comparison the slices were stained with hematoxylin/eosin. Macrophages and bacteria were detected with anti-CD68 and anti-Staphylococcus aureus specific antibodies using immunofluorescence.

Results and Discussion: In all animals distinct muscle abscesses could be generated. In the area of macrophage infiltration at the rim of the abscesses as demonstrated by anti-CD68 immunofluorescence, high uptake of H-DG was noted (L/M 9.6 ± 5.1). Tc-UBI, as well as, F-UBI derivatives exhibited increased uptake in the abscess area (L/M: Tc-UBI 19-41: 3.7 ± 2.7; F-UBI 19-41: 5.4 ± 2.4; F-UBI 18-41: 6.9 ± 4.7), which was partly congruent with H-DG uptake. In none of the cases, however, increased uptake of any of the UBI-derivates could be detected in areas which were highly positive for Staphylococcus aureus using immunofluorescence.

Conclusion: Neither ^{99m}Tc-UBI nor ¹⁸F- labelled Ubiquicidine derivatives showed specific uptake in Staphylococcus aureus in-vivo. Therefore, UBI derivatives appear not to be useful for discrimination between bacterial infection and unpecific inflammation.

Keywords: Tc-UBI, F-18-UBI, Inflammation

P349 IMAGING OF SECONDARY THALAMIC LESIONS WITH cis-4-(¹⁸F)FLUORO-D-PROLINE FOLLOWING FOCAL CORTICAL ISCHEMIA IN RATS**D. SALBER¹, K. HAMACHER², G. STOFFELS³, D. PAULEIT³, H.H. COENEN², K. ZILLES³ and K.J. LANGEN³**

¹C. & O. Vogt Institute of Brain Research, Düsseldorf University Hospital, Düsseldorf, Germany; ²Institute of Neurosciences and Biophysics-Nuclear Chemistry, Forschungszentrum Jülich, GmbH, Jülich; ³Institute of Neurosciences and Biophysics-Medicine, Forschungszentrum Jülich, GmbH, Jülich, Germany

Introduction: The amino acid cis-4-[¹⁸F]fluoro-D-proline (D-cis-FPro) exhibits preferred uptake into the brain compared with its L-isomer but the mechanisms of uptake and the clinical potential of this tracer are yet unknown. In this study we explored the cerebral uptake pattern of D-cis-FPro in rats with focal cortical infarctions.

Experimental: Focal cortical infarctions were induced in different areas of the cortex of 16 CDF-Fisher rats by photothrombosis (PT). At variable time points (3 days - 4 weeks) after PT the rats were injected intravenously with D-cis-FPro. For comparison, 8 rats were injected simultaneously with [³H]deoxyglucose (DG), 2 rats with [³H]PK11195, a ligand for peripheral benzodiazepine receptors, and 3 rats with L-[³H]-methionine (MET). Two hours after tracer injection coronal cryosections of the brains were produced and evaluated by dual tracer autoradiography. Lesion to brain ratios (L/B) were calculated by dividing the maximal uptake in areas with increased tracer uptake by the mean uptake in normal brain tissue. Histological slices were stained by cresyl violet, supplemented by immunostainings for glial fibrillary acidic protein (GFAP), CD68 for macrophages and OX42 for microglia in selected cases.

Results and Discussion: High uptake of D-cis-FPro was found in the demarcation zone of the cortical infarctions (L/B 11.4 ± 4.6) with an uptake pattern which resembled that of increased DG uptake (L/B 3.2 ± 1.2). Immunostaining for CD68 was positive in these areas indicating uptake in macrophages. A striking finding, however, was the uptake of D-cis-FPro in ipsilateral thalamic nuclei and the corpus striatum (L/B 6.6 ± 2.0). The involved thalamic nuclei varied with the site of the cortical lesion, i.e. only those nuclei were labelled which are sources of thalamo-cortical projections connecting them with their specific target region in the cerebral cortex. No major abnormalities were seen in the corresponding DG, MET and [³H]PK11195 autoradiograms as well as in histology and immunostainings of the thalamic nuclei with abnormal D-cis-FPro uptake.

Conclusion: D-cis-FPro appears to be a sensitive PET tracer to detect retrograde degeneration of thalamic nuclei and the basal ganglia after cortical injury. The uptake mechanism of D-cis-FPro in degenerating neurons or associated cell remains to be elucidated.

Keywords: D-Cis-F-Proline, Brain, Infarction

P350 DIMINISHED CU-ATSM HYPOXIA SELECTIVITY AND ITS RELATION TO FATTY ACID SYNTHASE EXPRESSION IN PROSTATE TUMORS

A.L. VAVERE and J.S. LEWIS

Division of Radiological Sciences, Washington University School of Medicine, St. Louis, MO, USA

Introduction: The validity of Cu-ATSM as a hypoxia imaging agent has been demonstrated in vitro, in vivo, and in humans, but there is concern in regards to its ability to delineate hypoxia in **prostate** tumors. Other groups have reported data in prostate tumor lines that did not support the use of Cu-ATSM, at times finding a negative correlation of uptake to oxygen levels. It is known that other physiological changes caused by hypoxia could affect the cellular redox balance regardless of oxygen concentration. For example, as a defense mechanism in prostate cancer cells, the fatty acid synthesis (FAS) pathway harnesses its oxidizing power for improving the redox balance despite conditions of extreme hypoxia. Although it is minimally expressed endogenously, FAS has been found to be over-expressed in prostate carcinomas. In this study, C75 (an inhibitor of fatty acid synthesis) was used to inhibit FAS activity, thereby overcoming the ability of FAS to offset the redox balance of a hypoxic cell therefore increasing uptake of Cu-ATSM.

Experimental: For each prostate tumor model, cells in suspension were maintained at 37°C in a water bath while constantly humidified by an anoxic gas mixture (95% N₂, 5% CO₂). During a 1 hour equilibration period, one flask was treated with C75 (100 mM) while the other served as a control. After equilibration, 100 μCi ⁶⁴Cu-ATSM was added to each flask. At various timepoints from 1-60 minutes, 200 mL of cell suspension was removed via pipet in triplicate, and the cells were separated from media and counted in a gamma counter to calculate percent uptake. FAS expression of each tumor line was measured using a FAS-detect™ ELISA kit (FASgen, Inc). These values were normalized by protein concentration as determined by BCA, resulting in a ratio with units of ng FAS/mg protein.

Results and Discussion: Inhibition of FAS with C75 resulted in a dramatic increase in ⁶⁴Cu-ATSM uptake into prostate tumor cells in vitro under anoxic conditions. The treated cells demonstrated higher uptake values of 20.9 ± 3.27, 103.0 ± 32.6, 144.2 ± 32.3, and 200.1 ± 79.3% over control values for LAPC-4, PC-3, LNCaP, and 22Rv1 prostate tumor cell lines after 15 minutes. Quantification of FAS expression, by ELISA, resulted in values of 0.00438 ± 0.00024, 0.00832 ± 0.00038, 0.01877 ± 0.00092, and 0.02679 ± 0.00224 ng/mg for LAPC-4, PC-3, LNCaP, and 22Rv1, respectively. As expected, a correlation is seen (R² = 0.9117) with FAS expression plotted against % change in ⁶⁴Cu-ATSM uptake with C75 treatment.

Conclusion: Although Cu-ATSM has clinical relevance in the imaging of hypoxia in numerous tumor types, its application to the imaging of prostate cancer may be limited by the cellular expression of FAS.

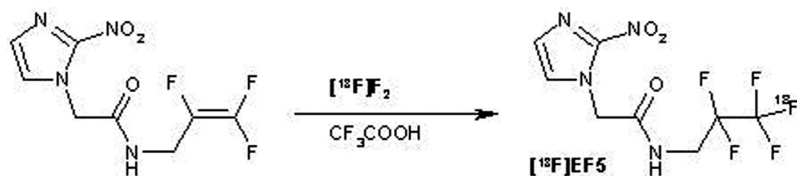
Acknowledgement: Financial support: DOD (PC040435) and NIH (F32CA110422-1).

Keywords: Cu-ATSM, Fatty Acid Synthase, Hypoxia, C75

P351 ANALYSIS OF ^{18}F -LABELLED METABOLITES OF (^{18}F)EF5 IN PATIENTS WITH HEAD AND NECK CANCERO. ESKOLA¹, T. GRONROOS¹, S. FORSBACK¹, M. HAAPARANTA¹, G. KOMAR¹, M. SEPPANEN¹, H. MINN² and O. SOLIN¹¹Turku PET Centre, Turku, Finland; ²Department of Oncology and Radiotherapy, Turku University Central Hospital, Turku, Finland

Introduction: We have recently synthesised and evaluated [^{18}F]-2-(2-nitro-1[*H*]-imidazol-1-yl)-*N*-(2,2,3,3,3-pentafluoropropyl)-acetamide ([^{18}F]EF5) as a radiotracer for imaging tumour hypoxia with PET. The aim of this study was to analyse radioactive metabolites of [^{18}F]EF5 from human plasma and urine samples.

Experimental: [^{18}F]EF5 was synthesized by electrophilic fluorination using high specific radioactivity [^{18}F]F₂ gas as labelling reagent. [^{18}F]EF5 was purified with semi-preparative HPLC and formulated for injection in physiological saline. [^{18}F]EF5 was intravenously injected into patients (n = 8) with head and neck squamous cell carcinomas (HNSCC). Seven arterial blood (5 - 180 min) and two urine (80 and 180 min) samples were collected during PET scan. Plasma was separated from whole blood and the plasma proteins precipitated before samples were applied on a silica HPTLC plate. [^{18}F]EF5 added to nonradioactive deproteinised human plasma was used as a standard. The HPTLC plate was developed in chloroform/methanol (70:20), dried and exposed to an imaging plate for 4 h. The plate was scanned for radioactivity with a Fuji BAS 1800 device and the data was analysed for formed ^{18}F -labelled metabolites.



Results and Discussion: The radiochemical yield of [^{18}F]EF5, decay corrected to the end of bombardment and based on the initial [^{18}F]F⁻ radioactivity (23 - 32 GBq at EOB), was in average $2.9 \pm 0.7\%$. The amount of purified [^{18}F]EF5 varied from 406 MBq to 798 MBq at the end of synthesis. The SA of [^{18}F]EF5, decay corrected to the end of synthesis, varied from 4.0 to 10.8 GBq/ μmol and was in average 6.9 ± 1.8 GBq/ μmol . Radiochemical purity exceeded 98.5% and chemical purity exceeded 95%, as analyzed with analytical HPLC. Synthesis time was 60 minutes. Essentially no ^{18}F -labelled metabolites of [^{18}F]EF5 were formed in plasma, as monitored up to 180 min after injection. In urine, a metabolite fraction representing about 20% of the total radioactivity was seen at 180 min after injection. This amount varied slightly between the patients. The share of protein-bound [^{18}F]EF5 remained constant throughout a 180 min study and was around 40%. Overall, our results confirm previous results with the unlabelled compound, that EF5 is very stable *in vivo*.

Conclusion: Our results show that no metabolite correction for the input function is needed in [^{18}F]EF5-PET.

Keywords: [^{18}F]EF5, Metabolite, Electrophilic, [^{18}F]F₂, Cancer

P352 ^{177}Lu -EDTMP AS A VIABLE AGENT FOR BONE PAIN PALLIATION

S. BANERJEE, T. DAS, S. CHAKRABORTY, H.D. SARMA and M. VENKATESH

Radiopharmaceuticals Division, Bhabha Atomic Research Centre, Mumbai, Maharashtra, India

Introduction: Agents labeled with β^- emitting radioisotopes such as, ^{153}Sm -EDTMP, $^{89}\text{SrCl}_2$ and ^{186}Re -HEDP offer an attractive therapeutic modality in palliative care of painful bone metastases. Comparatively shorter half-lives of ^{153}Sm and ^{186}Re and limited production capacity of ^{89}Sr are the factors posing practical limitations in their widespread use. ^{177}Lu with its favorable decay characteristics [$T_{1/2}=6.73$ d, $E_{\beta\text{max}}=496$ keV, $E_{\gamma}=208$ keV] and its large scale production feasibility using natural Lu target can be considered as an attractive radionuclide for developing bone pain palliatives. The comparatively longer $T_{1/2}$ of ^{177}Lu provides logistic advantages, a particularly important consideration in countries having limited isotope production facilities. The distinct advantage of the low energy β^- emission of ^{177}Lu provides less radiation dose burden to the bone marrow. ^{153}Sm -EDTMP being an approved agent for this purpose, provides insight towards designing an analogous agent using ^{177}Lu .

Experimental: ^{177}Lu was produced by irradiation of natural Lu_2O_3 at a thermal neutron flux of 6×10^{13} n/cm².s for 21 d. EDTMP was synthesized in-house. In a typical optimized radiolabeling protocol, 0.1 mL of $^{177}\text{LuCl}_3$ solution (~10 mCi) was added to 35 mg of EDTMP in 0.4 mL 0.5 M NaHCO_3 buffer (pH 9). The pH of the reaction mixture was maintained ~7 after the addition of 0.5 mL of normal saline. The mixture was incubated at RT for 30 min. The radiochemical purity was determined by PC in $\text{NH}_3:\text{EtOH}:\text{H}_2\text{O}$ (1:10:20 v/v) and paper electrophoresis. Bioevaluation and imaging studies were carried out in Wistar rats and New Zealand white rabbits.

Results and Discussion: ^{177}Lu was produced with a specific activity of 300 mCi/mg and 99.98% radionuclidic purity. ^{177}Lu -EDTMP was prepared in high yield and radiochemical purity (>99%) which was retained upto 30 d post-preparation, indicative of its high in-vitro stability at RT. 1.74±0.30% of injected activity was observed in per g of femur at 3 h p.i. with rapid blood clearance and minimal uptake in any other major organ/tissue in Wistar rats. Scintigraphic images recorded in Wistar rats and New Zealand white rabbits (fig 1) also demonstrated significant skeletal uptake with insignificant retention of activity in other vital organs.

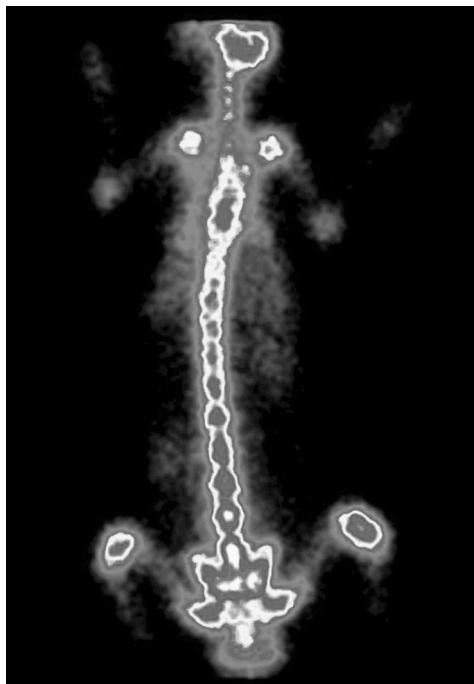


Fig. 1

Conclusion: ^{177}Lu -EDTMP prepared indigenously showed promising features in bioevaluation studies in animal models and could emerge as a viable bone pain palliative following the completion of successful human clinical trials.

Keywords: Lu-177, EDTMP, Bone Pain Palliation

P353 RADIOLABELLING AND EVALUATION OF A NOVEL IMAGING AGENT FOR HYPOXIC TISSUE IN STROKE

C.L. FALZON^{1,2,3}, U. ACKERMANN^{1,3}, J.M. WHITE², H.J. TOCHON-DANGUY^{1,3}, A.M. SCOTT¹, N. SPRATT³ and D. HOWELLS³¹Centre for PET, Austin Health, Heidelberg, Victoria, Australia; ²School of Chemistry/BIO21, The University of Melbourne, Parkville, Victoria, Australia; ³Department of Medicine, The University of Melbourne, Heidelberg, Victoria, Australia

Introduction: Hypoxia is of great significance in neurology and oncology. Fluoromisonidazole (FMISO) labelled with ¹⁸F, has been used with PET in humans for the identification of hypoxic tissue in stroke [1]. However, FMISO suffers from low cellular uptake into hypoxic tissue and slow clearance from normal cells, requiring long periods between injection and imaging; hence, the need to develop imaging agents with improved pharmacokinetics.

Experimental: We have recently reported the synthesis of two sulfoxide containing nitrogen mustards, labelled with ¹⁸F via a simple halogen exchange, as potential new imaging agents [2] (Figure 1). Evaluation studies in-vivo have been performed in a rat stroke model using the MCAO occlusion technique [3].

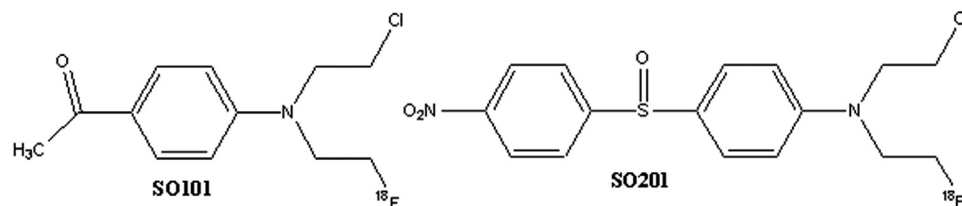


Fig. 1. Chemical structures of SO101 and SO201.

Results and Discussion: Uptake in the stroke affected hemisphere could be observed 1h and 2 h post tracer injection and was compared to the FMISO standard. Lipophilicity measurements of both compounds (SO101 and SO201) showed them to be more lipophilic than FMISO thus potentially crossing the blood brain barrier more readily.

Conclusion: Biodistribution and initial uptake studies in our rat stroke model showed that both tracers have potential as imaging agents in stroke. In particular, SO201 shows faster and higher uptake in the ischemic penumbra than FMISO.

References: [1] T.Hirano, S.J. Read, D.F. Abbott, J.G. Chan, J. Sachinidis, H.J. Tochon-Danguy, G.F. Egan, C.F. Bladin, A.M. Scott, W.J. McKay, G.A. Doonan, Identifying Ischemic Stroke using PET and ¹⁸F-Fluoromisonidazole, *Neurology*, 51, **1998**, 6117-6121. [2] C.L. Falzon, U. Ackermann, N. Spratt, H.J. Tochon-Danguy, J. White, D. Howells, A.M. Scott, "F-18 labelled N,N-Bis-haloethylamino-phenylsulfoxides – A new class of compounds for the imaging of hypoxic tissue" *J. Labelled Cpd. Radiopharm.* **2006**, 49: 1089-1103 [3] N.J. Spratt, J. Fernandez, M. Chen, S. Rewell, S. Cox, L. Raay, L. Hogan, D.W. Howells, Modification of method of thread manufacture improves stroke induction rate and reduces mortality after thread-occlusion of the middle cerebral artery in young or aged rats. *Journal of Neuroscience Methods*, **2006**, 155(2):285-90.

Keywords: Hypoxia, Stroke, Biodistribution, Halogen Exchange, Fluorination

P354 PRE-, EX- AND IN-VIVO EVALUATION OF (⁶⁸Ga)-EDTMP

M. MITTERHAUSER^{1,2}, S. TOEGEL^{1,2}, W. WADSAK¹, R.R. LANZENBERGER³, L.-K. MIEN^{1,2}, C. KUNTNER⁴, T. WANER⁴, D.E. ETLINGER¹, H. EIDHERR¹, R. DUDCZAK¹ and K. KLETTER¹

¹Nuclear Medicine, Medical University of Vienna, Vienna, Austria; ²Pharmaceutical Technology and Biopharmacy, University of Vienna, Vienna, Austria; ³General Psychiatry, Medical University of Vienna, Vienna, Austria; ⁴Department of Radiopharmaceuticals, Austrian Research Centres Seibersdorf, Seibersdorf, Austria

Introduction: The present study was designed to develop a simple preparation method for [⁶⁸Ga]-EDTMP and to evaluate the applicability of [⁶⁸Ga]-EDTMP as a potential PET bone imaging agent using *pre-vivo*, *ex-vivo* and *in-vivo* models.

Experimental: [⁶⁸Ga]-EDTMP was prepared using [⁶⁸Ga]-gallium chloride eluted from the ⁶⁸Ge/⁶⁸Ga-generator and commercially available Multibone[®] kits.

Binding affinity to bone compartments was evaluated using a recently established *pre-vivo* model. [1,2] Powdered hydroxyapatite and human bone allografts were incubated for 3 hours and filtered to obtain binding. *In-vivo* (microPET) and *ex-vivo* experiments were performed in mice and compared with results obtained with [¹⁸F]-fluoride.

Results and Discussion: [⁶⁸Ga]-EDTMP was accessible via simple kit preparation and predominantly accumulated in bone tissue *in-vivo*, *ex-vivo* and *pre-vivo*. Binding to mineral bone was irreversible and low binding was observed in the organic compartment of bone (table 1). *In-vivo* microPET evaluation revealed predominant uptake in bone with renal excretion. Compared to [¹⁸F]-fluoride, uptake was lower and PET image quality was reduced.

Radiotracer	Filter value	Hydroxyapatite	Human Bone	Decalcified Bone
[⁶⁸ Ga]-EDTMP	5.6±1.5	4.29±2.74	5.44±1.99	1.08±1.89
[⁶⁸ Ga]-gallium chloride	4.9±1.5	59.2±7.1	68.6±8.0	40.3±7.8

Binding of [⁶⁸Ga]-EDTMP and [⁶⁸Ga]-gallium chloride on filter, 3 mg hydroxyapatite (HA), bone allograft (Co) and decalcified bone allograft (D-Co) after 120 min. Each value represents the arithmetic mean of 5 experiments with each measurement performed in triplicate.

Conclusion: From the present evaluation the advantage of [⁶⁸Ga]-EDTMP over [¹⁸F]-fluoride is not apparent and the future clinical perspective of [⁶⁸Ga]-EDTMP remains speculative.

References: [1] Mitterhauser M, Tögel S, Wadsak W, Mien LK, Eidherr H, Wiesner K et al. Binding studies of [¹⁸F]-fluoride and Polyphosphonates radiolabelled with [¹¹¹In], [^{99m}Tc], [¹⁵³Sm] and [¹⁸⁸Re] on bone compartments: A new model for the pre vivo-evaluation of bone seekers? Bone 2004; 34:835-44. [2] Mitterhauser M, Toegel S, Wadsak W, Mien LK, Eidherr H, Kletter K et al. Binding studies of [¹⁸F]-fluoride and polyphosphonates radiolabelled with [⁹⁰Y], [^{99m}Tc], [¹¹¹In], [¹⁵³Sm] and [¹⁸⁸Re] on bone compartments: Verification of the pre-vivo model? Bone 2005;37:404-12.

Keywords: Bone, PET, Gallium-68, Fluorine-18, Bone Scan

P355 LIPID BIOSYNTHESIS AS A MARKER OF TUMOR THERAPY RESPONSE**E.R. BUTCH, P.S. SHERMAN, C. QUESADA and S.E. SNYDER**

Radiology, University of Michigan Medical School, Ann Arbor, MI, USA

Introduction: Studies have pointed toward the importance of lipid metabolism in cell membrane formation and cell proliferation, and to the potential of these processes as targets for both chemotherapy and imaging. [C-11]Acetate and [C-11]choline are both known to be incorporated into membrane phospholipids in tumors. As such, these radiopharmaceuticals can be used to monitor changes in lipid membrane biosynthesis in vivo. The studies presented here utilize a mouse model of radiotherapy for squamous-cell carcinoma to determine whether lipid biosynthetic activity is a useful marker for non-invasive therapy monitoring.

Experimental: SCC VII murine tumors were grown s.c. in C3H mice. Ten days after implantation, tumors were treated with 50 Gy of radiation using a modification of the methods of Fields, et al (Int J Radiation Onc Biol Phys (2000) 47:785-91). Tumor volumes were measured three times per week during the entire treatment protocol. At the end of radiotherapy, ex vivo dissection and counting experiments were performed using either [C-11]acetate or [C-11]choline. Mice were injected i.v. with 0.1-0.15 mCi of either [C-11]acetate or [C-11]choline. At 20 minutes post-injection of the PET radiotracer, mice were sacrificed by decapitation. Tumors were rapidly dissected, weighed and counted for carbon-11 activity and data were expressed as percent of injected radiotracer dose per gram of tissue. Untreated tumor-bearing mice were also examined as controls. Small animal PET was performed on a subset of animals before and after therapy. Mice were injected i.v. with 0.35 - 0.5 mCi of either [C-11]acetate or [C-11]choline and 60 min dynamic imaging was performed.

Results and Discussion: The mean [C-11]choline uptake in tumors after radiation therapy was significantly lower than controls ($p < 0.01$). Group mean differences in [C-11]acetate between treated and control tumors was not statistically significant ($p = 0.28$). Both radiotracers exhibited a modest correlation between radioactivity uptake and therapy-induced tumor regression ($r^2 = 0.55$ and 0.58). This correlation could not be accounted for by differences in tumor size; plots of tumor weight vs radiotracer uptake in control tumors showed no correlation or a small negative correlation ($r^2 = 0.33$ and 0.19). PET imaging of individual animals pre- and post-radiotherapy showed a 30-40% therapy-induced decrease in radiotracer accumulation in tumor with both [C-11]acetate and [C-11]choline.

Conclusion: Variations in tumor growth rate and response to therapy make comparisons of mean radiotracer concentration between treated and control tumors difficult. However, the intrasubject decrease in radiotracer accumulation is easily measurable by PET. Thus, measurement of tumor lipid biosynthesis is an attractive marker for assessing response to therapy.

Acknowledgement: UM Head & Neck Cancer S.P.O.R.E.

Keywords: Therapy Monitoring, Acetate, Choline, Small Animal Imaging, Lipid Biosynthesis

P356 *IN VIVO* EVALUATION OF ^{111}In -LABELED, AMINO ACID-MODIFIED PNA-PEPTIDE CONJUGATES IN SMALL LYMPHOCYTIC LYMPHOMA

F. JIA¹, B.S. BALAJI¹, F. GALLAZZI², S.Z. LEVER³, M. HANNINK⁴ and M.R. LEWIS¹

¹Veterinary Medicine and Surgery, University of Missouri, Columbia, MO, USA; ²Molecular Biology Program; ³Chemistry; ⁴Biochemistry

Introduction: The *B-cell lymphoma/leukemia-2 (bcl-2)* gene produces an apoptosis inhibitor overexpressed in many cancers. We have developed an ^{111}In -labeled peptide nucleic acid (PNA)-peptide conjugate targeting *bcl-2* expression (1, 2). Although tumor *bcl-2* expression in a mouse model of small lymphocytic lymphoma (SLL) was imaged by this conjugate, high kidney and liver accumulation could limit *in vivo* applications. In order to promote renal and hepatobiliary clearance, modified PNA monomers with neutral hydrophilic (serine, T_S) or negatively charged (aspartic acid, T_D) residues were synthesized (3) as substitutes for glycine at T¹⁴ in the PNA sequence.

Experimental: DOTA-anti-*bcl-2*-(T_S)-PNA-Tyr³-octreotate (**1**) and DOTA-anti-*bcl-2*-(T_D)-PNA-Tyr³-octreotate (**2**) were labeled with ^{111}In in 0.2 M ammonium acetate, pH 5.0, containing 0.1% Tween-80. The radiolabeled compounds were purified by RP-HPLC. SCID mice bearing Mec-1 human SLL xenografts were administered 10 μCi of ^{111}In labeled conjugates with 20 mg of lysine. Biodistributions were obtained from 1 to 48 h post-injection.

Results and Discussion: ^{111}In labeled **1** showed specific tumor uptake at 2.18% ID/g at 1 h and 1.56% ID/g at 48 h. Kidney uptake was 52.3% ID/g at 1 h but cleared by factor of 2.4 at 48 h. The tumor/blood ratio increased from 0.63 at 1 h to 57.2 at 48 h. Liver uptake was low (0.56-0.78% ID/g) at all time points. ^{111}In labeled **2** demonstrated slightly lower tumor uptakes (1.27% ID/g at 1 h and 1.01% ID/g at 48 h). Kidney uptake was 36.9% ID/g at 1 h and cleared by factor of 2.1 by 48 h. Liver uptake was about half that for **1** at all time points. In contrast, the parent all glycine conjugate showed tumor uptakes of 2.28% ID/g and 1.33% ID/g, kidney uptakes of 33.6% ID/g and 13.6% ID/g, and liver uptakes of 6.37% ID/g and 6.07% ID/g at 1 and 48 h, respectively.

Conclusion: In summary, two amino acid-modified PNA conjugates targeting *bcl-2* gene expression were synthesized and labeled with ^{111}In . Biodistribution studies showed both compounds had specific tumor uptake. Kidney uptakes were similar to the unmodified peptide-PNA conjugate, but significantly lower liver uptake ($p < 0.003$) was observed for both compounds. These modified ^{111}In labeled peptide-PNA conjugates are being compared to the parent compound for microSPECT/CT imaging of tumor *bcl-2* expression in mouse models of SLL.

References: [1] Jia, F., et al. *J. Nucl. Med.* **47**: 94P, 2006. [2] Jia, F., et al. *Technetium, Rhenium and Other Metals in Chemistry and Nuclear Medicine* **7**: 201-206, 2006. [3] Balaji, B.S., et al. *Bioconjugate Chem.* **17**: 551-558, 2006.

Acknowledgement: NIH Grant CA103130.

Keywords: Bcl-2, Peptide Nucleic Acid, In-111, MicroSPECT/CT, Small Lymphocytic Lymphoma

P357 IN VIVO PHARMACOKINETICS OF A¹¹¹In-RADIOLABELED SMALL MOLECULE TARGETING LFA-1 EXPRESSION**J.P. NOREBERG¹, T.L. ANDERSON¹, T.K. NAYAK^{1,2}, R.B. PORIA³, J.L. ERION⁴, H.J. HATHAWAY², C.R. WAGNER⁵, J.B. ARTERBURN⁶ and R.S. LARSON²**

¹Radiopharmaceutical Sciences, College of Pharmacy, University of New Mexico, Albuquerque, NM, USA; ²School of Medicine, University of New Mexico, Albuquerque, NM, USA; ³Radiology, University of Pennsylvania, Philadelphia, PA, USA; ⁴BioSynthema Inc., Saint Louis, MO, USA; ⁵Medicinal Chemistry, University of Minnesota, Minneapolis, MN, USA; ⁶Chemistry and Biochemistry, New Mexico State University, Las Cruces, NM, USA

Introduction: Leukocyte function-associated antigen-1 (LFA-1) is constitutively expressed on leukocytes, but over expressed on most lymphomas and leukemias. We synthesized a derivative of BIRT 377 (butylamino-NorBIRT), an allosteric inhibitor of LFA-1. The cellular binding assays with butylamino-NorBIRT have given promising results. We have now incorporated a radiometal, Indium-111 (0.171MeV and 0.245 MeV gamma emissions), into the compound to investigate its tracer potential and in vivo binding.

Experimental: Indium-111 was incorporated into the butylamino-NorBIRT using 1,4,7,10-tetraazacyclododecane-N,N,N,N-tetraacetic acid (DOTA) as a chelator. Greater than 95% incorporation yield was obtained. The *in vivo* characterization of the ¹¹¹In DOTA-butylamino-NorBIRT was determined using pharmacokinetics and biodistribution studies on normal, female C57 bl/6 mice. This was accomplished by injecting 7Ci/g in mice with the ¹¹¹In DOTA-butylamino-NorBIRT. The animals were sacrificed at 1, 6, and 24 hours to allow for distribution, localization, and clearance. Both target and non-target organs were harvested, weighed, and washed, to determine the radioactivity per gram of tissue (percent-injected dose per gram of tissue, %ID/g).

Results and Discussion: At 1 hour post injection 2.537%ID/g was seen in the heart as compared to 0.518%ID/g at 6 hours and 0.086%ID/g at 24 hours, 7.856%ID/g in the blood compared to 1.332% ID/g and 0.076%ID/g, 6.745%ID/g in the liver compared to 3.350% ID/g and 0.534%ID/g, and in the lungs 6.726%ID/g compared to 1.486%ID/g and 0.715%ID/g, all respectively. No significant difference was seen in non target organs such as the brain 0.220%ID/g at 1 hour compared to 0.041% ID/g at 6 hours and 0.012%ID/g at 24 hours. All the data is normalized and decay corrected. The results indicate significant clearance from all tissues over 24 hours. It is promising especially with delayed imaging, to obtain a higher target to background ratio thereby better imaging of metastasized masses.

Conclusion: The results obtained indicated that butylamino-NorBIRT can be a potential imaging agent for many types of leukemias and lymphomas. Further in vivo studies will be conducted in a mouse tumor model.

Acknowledgement: Acknowledgement: WM KECK Foundation, UNM-LANL Joint Sciences and Technology Initiatives.

Keywords: Indium-111, Leukocyte Function-Associated Antigen-1 (LFA-1), Butylamino-NorBIRT

P358 COMPARISSON OF ^{99m}Tc -DMSA-V, ^{99m}Tc -MIBI AND ^{18}F FDG FOR MELANOMA DETECTIONF.L.N. MARQUES¹, A. RADIN¹, A.H. OTAKE², J.B.S. RODRIGUES¹, R. CHAMMAS² and C.A. BUCHPIGUEL¹¹Centro de Medicina Nuclear, Faculdade de Medicina – Universidade de São Paulo, São Paulo, SP, Brazil; ²Laboratório de Oncologia, Faculdade de Medicina da Univ. de São Paulo, São Paulo, SP, Brazil

Introduction: Melanoma is a highly malignant tumor whose incidence is continuously rising worldwide. Despite its topography, which makes diagnosis simpler, melanomas are highly aggressive tumors and it is not uncommon to observe lymph node metastasis at diagnosis. Therefore, adequate treatment depends on accurate staging of the disease. Protocols assessing the value of studying the sentinel lymph node are still in debate in the literature. Among the image-based alternative methods for tumor staging, whole-body scintigraphy or lymphoscintigraphy have been used for detection of metastatic lesions, using [^{99m}Tc]technetium colloidal radiopharmaceuticals. In this report we compared ^{99m}Tc -DMSA-V, ^{99m}Tc -MIBI and [^{18}F]FDG regarding their uptake by melanoma tumors.

Experimental: ^{99m}Tc -DMSA-V and ^{99m}Tc -MIBI were generated using in house kits and [^{18}F]FDG was purchased from IPEN-Brazil. 5×10^5 B16F10 murine melanoma cells were injected subcutaneously in C57/bl6 mice. After 10 days, radiopharmaceutical were injected, groups of 3 animals were anesthetized and sacrificed at 15, 60 and 120 minutes after radiopharmaceutical injection. Organs were removed, weighted and uptaken radioactivity was measured in a well counter. Results were summarized as concentration of the radiopharmaceuticals in tumor/muscle, tumor/blood and tumor/lung, and were expressed as % dose/organ wet weight. Radiopharmaceuticals were imaged in gamma camera, 120 minutes after injection.

Table 1. Tumor/muscle rate expressed as media \pm SD (n=3)

	15 min	60 min	120 min
^{99m}Tc -MIBI	0.29 \pm 0.23	0.22 \pm 0.18	0.15 \pm 0.04
^{99m}Tc -DMSA-V	3.78 \pm 1.34	2.87 \pm 0.85	3.41 \pm 1.17
[^{18}F]FDG	2.76 \pm 0.60	2.56 \pm 0.47	2.24 \pm 0.37

Table 2. Tumor/blood rate expressed as media \pm SD (n=3)

	15 min	60 min	120 min
^{99m}Tc -MIBI	0.94 \pm 0.25	2.40 \pm 0.88	3.17 \pm 0.94
^{99m}Tc -DMSA-V	0.98 \pm 0.68	0.75 \pm 0.20	1.31 \pm 0.40
[^{18}F]FDG	1.25 \pm 0.47	12.21 \pm 2.00	26.93 \pm 2.62

Table 3. Tumor/lung rate expressed as media \pm SD (n=3)

	15 min	60 min	120 min
^{99m}Tc -MIBI	0.32 \pm 0.07	0.39 \pm 0.06	0.21 \pm 0.05
^{99m}Tc -DMSA-V	1.41 \pm 1.08	1.01 \pm 0.46	1.24 \pm 0.31
[^{18}F]FDG	0.95 \pm 0.35	3.29 \pm 0.91	3.56 \pm 0.98

Conclusion: ^{99m}Tc -MIBI was not an appropriate radiopharmaceutical for melanoma detection, as compared to [^{18}F]FDG. In turn, ^{99m}Tc -DMSA-V has potential application for detection of melanoma, as compared to [^{18}F]FDG, taking into account tumor/muscle and tumor/lung uptake rates and image are in agreement with this propositions.

Keywords: Melanoma, Detection, ^{99m}Tc -DMSA, ^{99m}Tc -MIBI, [^{18}F]FDG

P359 EVALUATION OF ¹⁷⁷Lu-LABELED DOTMP AND EDTMP**C.S. CUTLER¹, J.N. BRYAN⁴, M. CHANDIA³, D.J. IRWIN¹, H.P. ENGELBRECHT¹, T. ROLD², J.C. LATTIMER⁴, T. HOFFMAN², C.J. HENRY^{2,3} and A.R. KETRING¹**

¹Research Reactor Center, University of Missouri-Columbia, Columbia, MO, USA; ²Department of Internal Medicine, Hematology and Oncology, University of Missouri-Columbia, Columbia, MO, USA; ³Chilean Nuclear Energy Commission, Santiago, Chile; ⁴Department of Veterinary Medicine and Surgery, University of Missouri-Columbia, Columbia, MO, USA

Introduction: The intent is to evaluate the *in vivo* behavior of ¹⁷⁷Lu-DOTMP and ¹⁷⁷Lu-EDTMP as possible agents for palliation of metastatic bone pain. Phosphonates such as EDTMP and DOTMP can be labeled in high yields of 99% with the radioisotope ¹⁷⁷Lu. The complexes remain stable for at least 14 days at room temperature. The radioisotope, ¹⁷⁷Lu, has nuclear properties that make it suitable for use in palliative therapy of bone metastasis including: a large cross section that allows for production at most moderate flux reactors, a relatively long half life which gives ¹⁷⁷Lu a longer effective shelf life and increases its range of distribution, and a lower energy beta emission which lowers the potential for treatment-related organ toxicity. Because of this, ¹⁷⁷Lu labeled phosphonates are being considered for bone pain palliation.

Experimental: Biodistribution studies of the ¹⁷⁷Lu complexes were conducted using CF1 normal mice. Studies were performed by injecting 5 μCi in 100 μL of saline via the tail vein. Four to five animals were analyzed per time point at 0.25, 0.5, 2, 4, and 24 hr post-injection. Tissues and fluids were collected and the radioactivity quantitated to calculate the percent injected dose per organ (%ID) and the percent injected dose per gram (%ID/g). The systemic toxicity of ¹⁷⁷Lu-DOTMP is also being evaluated in normal dogs at a dose of 0.22 mCi/kg. ¹⁷⁷Lu-DOTMP was administered intravenously and blood collection, urinalysis, and bone marrow aspiration/biopsy have been performed out to 28 days.

Results and Discussion: Biodistribution studies of ¹⁷⁷Lu- EDTMP and DOTMP in normal mice showed significant skeletal uptake, with rapid blood clearance and minimal uptake in other major organs. The observed skeletal uptake at 4 hr post injection was 16.12%ID/g and 11.33%ID/g for DOTMP and EDTMP respectively. For both DOTMP and EDTMP, approximately 60% of the injected dose was cleared through the kidneys into the urine by 30 min post injection. No Toxic effects were observed in the dogs at 28 days.

Conclusion: ¹⁷⁷Lu-DOTMP was easier to formulate and exhibited higher skeletal uptake in comparison with ¹⁷⁷Lu-EDTMP. Based on these results ¹⁷⁷Lu-DOTMP is being further evaluated in normal dogs and initial results indicate less pronounced hematologic toxicity than that which occurs after ¹⁵³Sm-EDTMP administration. Based on these results, ¹⁷⁷Lu should be considered as a possible alternative radioisotope for bone pain palliation.

Acknowledgement: IAEA Fellowship CH105001.

Keywords: Lutetium-177, DOTMP, EDTMP, Bone Pain Palliation, Lutetium-177 Phosphonates

P360 A MODULAR PLATFORM FOR TARGETED IMAGING BASED ON A VIRAL CAPSID: DESIGN, SYNTHESIS, AND PRELIMINARY EVALUATION

J.M. HOOKER¹, J.P. O'NEIL², S.E. TAYLOR², D.W. ROMANINI¹ and M.B. FRANCIS^{1,3}

¹Department of Chemistry, University of California, Berkeley, CA, USA; ²Department of Molecular Imaging and Neuroscience; ³Material Sciences Division, Lawrence Berkeley National Laboratory, Berkeley, CA, USA

Introduction: The availability of well-defined nanoscale materials offers exciting new approaches for the diagnosis and treatment of disease.¹ In contrast to small molecule pharmaceuticals, the large dimensions of these structures confer extended blood circulation times and the ability to construct multifunctional devices that integrate targeting, imaging, and therapeutic components. However, these complex materials have been difficult to produce in practice due to the lack of nanoscale scaffolds that offer biocompatibility, low polydispersity, flexible synthetic modification in multiple locations, and high stability in biological settings. In order to incorporate all of these design elements, we have developed methods to convert the protein shell of a virus into versatile imaging agents that can target specific tissue types or disease markers *in vivo*, Figure 1.

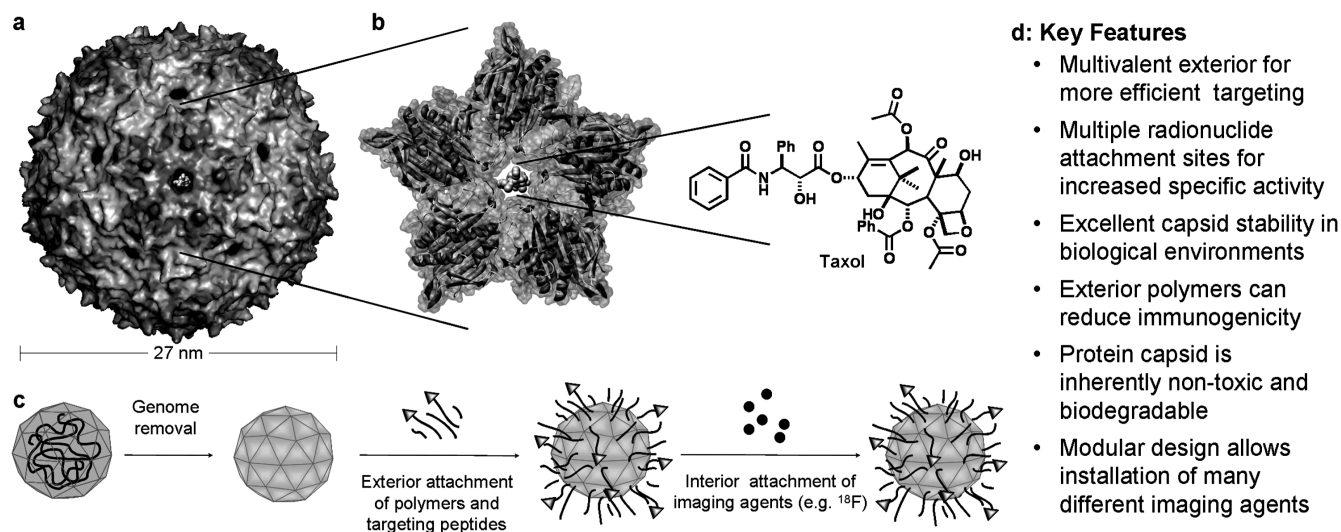


Figure 1. Construction of nanoscale diagnostic imaging agents from bacteriophage MS2. (a) The intact protein capsid assembles from 180 copies of a coat protein, producing a 27 nm hollow shell that possesses 32 “holes” that are 2 nm in diameter. (b) Close-up of a pentameric section shows the pore in relation to Taxol, an anticancer drug. (c) RNA genome is removed from the capsid and peptides targeting specific tissue types will be installed on the exterior surface. Positron emitting ¹⁸F nuclei is then installed on the interior surface. Key features of this system are summarized in (d).

Experimental: 3-Formyl-4-nitroaniline was synthesized from *m*-nitrobenzaldehyde (21%, 5 steps), diazotized, and reacted with mtMS2. Condensation with a bis-alkoxyamine rendered capsids reactive toward [¹⁸F]fluorobenzaldehyde (65-70% RCY from [¹⁸F]Cs₂CO₃ and 4-formyl-*N,N,N*-trimethylanilinium triflate) (15-25% RCY protein labeling).

Results and Discussion: Our chemical strategy for the use of bacteriophage MS2 relies on the site selective modification of a uniquely reactive tyrosine (Y85).² A new diazonium salt precursor was synthesized in order to introduce a bioorthogonal reactive handle on the interior surface of the hollow protein shell. This aldehyde can be further elaborated with amino-oxy functional groups, affording stable oxime linkages. This modular strategy allows the introduction of up to 180 copies of virtually any small-molecule imaging or therapeutic agent. As an initial demonstration of the potential of these nanoscale imaging agents, we have applied our strategy to incorporate n.c.a. [¹⁸F]fluorobenzaldehyde into this scaffold. Details of the [¹⁸F] capsid synthesis, purification, biodistribution, and imaging studies will be presented.

References: [1] Garcea, R.L.; Gissmann, L. *Curr Opin Biotech* **2004**, *15*, 513. [2] Hooker, J.M.; Kovacs, E.W.; Francis, M.B. *J Am Chem Soc* **2004**, *126*, 3718.

Acknowledgement: This work was sponsored by the Office of Science, Department of Energy, contract No. DE-AC03-76SF00098.

Keywords: Virus, Nanomaterial, PET, F-18, Protein Modification

P361 MODELLING OF PET LIGAND/MEMBRANE INTERACTIONS

L. PARAMONOV¹, A. GEE^{1,2} and S.N. YALIRAKI¹¹Department of Chemistry, Imperial College London, London, United Kingdom; ²GSK Clinical Imaging Centre, Imperial College London, Hammersmith Hospital, London, United Kingdom

Introduction: The non-specific binding of PET ligands is a ubiquitous but poorly understood phenomenon. Better design rules for ligands can be obtained if the interaction of PET ligands with the membrane is explained, and in particular if the hypothesis that the non-specific binding of ligands involves lipid hydrolysis and degeneration of the membrane is tested (see [1]).

The interaction of PET ligands with the membrane occurs at a range of length and time scales that span orders of magnitudes from nanometres to microns, and, femtoseconds to minutes, even hours. Theoretical methods that can address the dynamic behaviour of such systems are currently not available. A typical atomistic-scale molecular dynamics simulation cannot span more than hundreds of nanoseconds or hundreds of nanometers.

We have developed a new Coarse-Grained (CG) theoretical methodology (see [2,3]) to investigate the role of the lipid membrane in the non-specific binding of PET ligands via molecular dynamics simulations that can overcome these problems.

Results and Discussion: In preliminary results, we have observed the crossing of the ligand inside the membrane. We can obtain the time it takes for this transition to occur as well as the diffusion of the ligand inside the membrane. The hydrophobic properties of the ligand, together with its size and shape can be used to tune this behaviour and hence the non-specific binding. It is possible to generalise the model to include proteins so that the competition with receptor binding can be explicitly observed in the future.

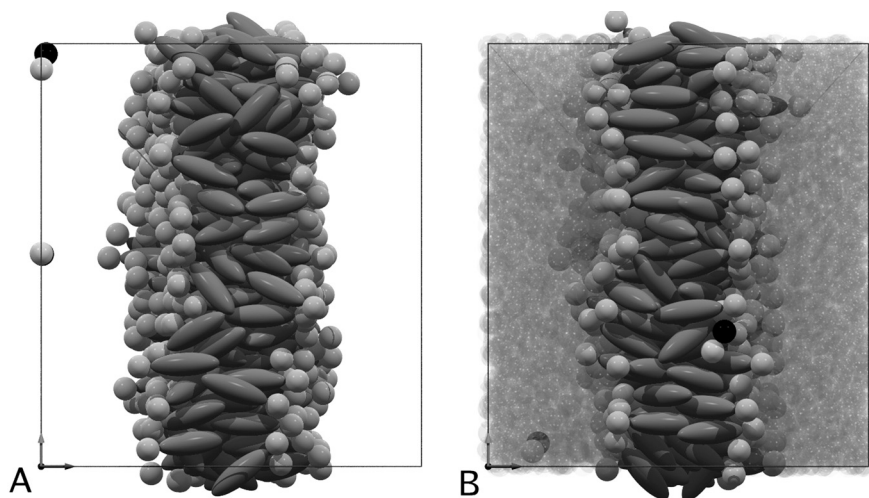


Fig. 1. The transition of CG ligands into the membrane interface. A: The initial position of the CG ligands with respect to a membrane sample at $t=0$ (the explicit solvent sites are not shown). B: Position of the CG ligand at the membrane interface after a short simulation.

References: [1] M. Baciuet al., "Degradative transport of cationic amphiphilic drugs across phospholipid bilayers", *Phil. Trans. R. Soc. A* (2006), Vol. 364, pp. 2597-2614. [2] L. Paramonov and S.N. Yaliraki, "Degradative transport of cationic amphiphilic drugs across phospholipid bilayers", *J. Chem. Phys.*, submitted, 2006. [3] L. Paramonov and S.N. Yaliraki, "Degradative transport of cationic amphiphilic drugs across phospholipid bilayers", *J. Chem. Phys.*, Vol.123, art. 194111, 2005.

Keywords: Membrane, Ligand, Interaction, Modeling, Coarse-Grain

P362 ¹¹C-METHYLATED LY2181308, AN ANTISENSE OLIGONUCLEOTIDE TO SURVIVIN: PART II-HUMAN DOSIMETRY CALCULATION

C.S. DENCE, R. LAFOREST, T.L. SHARP, R.H. MACH and M.J. WELCH

Radiology, Washington University School of Medicine, St. Louis, MO, USA

Introduction: We previously reported (J. Labl. Compd. Radiopharm. 2005:48:S161) the radiochemical synthesis and preliminary rodent biodistribution studies of [¹¹C] Me-LY2181308. This is an 18-mer antisense oligonucleotide of molecular weight ~ 6,400 Da, designed against survivin mRNA. We also reported the in vivo uptake in BALB/C mice with EMT-6 implanted tumors at 60 min post-injection. **Purpose:** The encouraging results, as evidenced by the relatively favorable tumor/blood and tumor/muscle ratios in previous studies, guided us to the next step of the evaluation process, the calculation of image-based human dosimetry.

Experimental: We determined the human radiation dose estimates based on the biodistribution of the radiotracer in baboon. Whole-body PET images were obtained in a total of three animals, one male and two females. Animal handling protocol was conducted accordingly to WUSM guidelines for the care and treatment of research animals. The animals were injected with an average of 7.9 mCi of [¹¹C] Me-LY2181308, the tracer biodistribution was followed in 4-8 scans during the 2 hours post-injection, followed by a transmission scan of 2-min per bed position. These values were used to calculate attenuation correction factors. The first scans were followed by a second injection of the tracer and the image acquisition resumed after ~ 3 hrs.

Results and Discussion: The dose limiting organ for [¹¹C] Me-LY2181308 appears to be the kidney with a radiation dose of 0.118 rad/mCi (32 μGy/Mbq). The second target organ is the liver with a radiation dose of 0.082 rad/mCi (22.1 μGy/Mbq). Based on these findings, an Effective Dose Equivalent of 23.4 mrem/mCi (6.72 μSv/MBq) which translates to an Effective Dose of 16.2 mrem/mCi (4.54 μSv/MBq) has been determined.

Conclusion: A complete evaluation of human dosimetry for [¹¹C] Me-LY2181308 was accomplished, thus facilitating the future use of this tracer in the clinical setting.

Acknowledgement: This work was supported by Eli Lilly and Company, Indianapolis, IN.

Keywords: Carbon-11, Oligonucleotides, Survivin